Description of Technology

3 February 2025

Table of Contents

1 Introduction

The Earthview BluBird gas monitoring system consists of the measuring and reporting instrument (the BluBird itself), the cloud-based computations that compute analyte concentrations and emission rates, and the cloud-based tools and human interactions that deliver the information to the customer.

This document provides a description of the Earthview BluBird monitoring system and the implementation of the system for purposes of meeting the periodic screening requirements in the New Source Performance Standards (NSPS) for oil and natural gas facilities. The BluBird system provides a 90% probability of detection of ≤5 kg/hr, making it suitable for quarterly or semiannual screenings as defined in tables 1 and 2 of the OOOOb regulations.

- Section 1: Introduction and workflow for the Earthview BluBird continuous monitoring system
- Section 2: Description of the technology, including the scientific theory, physical instrumentation, type of measurement and application, and potential limitations
- Section 3: Description of how Earthview's system converts air samples to methane concentrations
- Section 4: Description of how Earthview's system converts methane concentrations to mass emission rates, including performance assessments and probability of detection
- Section 5: Description of the security policies and data flow
- Section 6: References to supporting documentation discussed in this document

1.1 Description of Terms

Term	Definition
90% POD	Emission rate that is detectable 90% of the time.
ADED	Advancing Development of Emissions Detection. Continuous testing done by METEC.
Air zero calibration gas	Pure oxygen and nitrogen with impurities removed.

Term	Definition
AWS	Amazon Web Services.
Axetris LGD TDLAS	Laser Gas Detection Tunable Diode Laser Absorption Spectrometer manufactured by Axetris.
BluBird	Field instrument portion of the system. The device taking the in-situ measurements.
BluBird GMS	BluBird Gas Monitoring System, the entire system responsible for methane detection, quantification, and alerts.
BluBird v.1	Prototype version of the BluBird instrument (circa 2019-2021).
BluBird v.2	The current commercially-available version of the BluBird hardware (circa 2022-present).
BluBird v.3	The next version of the BluBird hardware (presently being designed).
CEMM	EPA Center for Environmental Measurement and Modeling.
CH_4	Methane.
Clean air	An air sample assumed to be free of elevated amounts of gas contaminants (aka, background air).
GMS	Gas Monitoring System.
CSU	Colorado State University.
field	The onsite location that is actively monitored by the BluBird GMS.
g	Grams. Measure of mass.

Term	Definition
g/m^3	Grams per cubic meter. Measure of concentration.
g/mol	Grams per mole. Molar mass.
g/s	Grams per second. Measure of mass flow rate.
GPAQS	Gridded Pad Analysis and Quantification System, the cloud based software of the system.
GPS	Global positioning system.
IoT	Internet of Things.
J	Joule. Measure of energy.
K	Kelvin. Measure of temperature. Kelvin = Celsius + 273.15.
kg/hr	Kilograms per hour. Measure of mass flow rate.
LDAR	Leak detection and repair.
LEL	Lower Explosive Limit.
LGD	Axetris LGD TDLAS.
m	Meters. Measure of distance.
m/s	Meters per second. Measure of speed.
MCFH	1000 cubic feet per hour. Measure of gas volume.
METEC	Methane Emissions Technology Evaluation Center. Testing facility sponsored by Colorado State University.
MOS	Metal oxide semiconductor.

Term	Definition
MOS 1/ gas1	Refers to one of three MOS sensors contained in the BluBird sensor chamber.
MOS 2/ gas2	Refers to one of three MOS sensors contained in the BluBird sensor chamber.
MOS 3/ gas3	Refers to one of three MOS sensors contained in the BluBird sensor chamber.
MOX	Metal oxide sensor.
node	An individual BluBird sensor unit.
OTA	Over the air.
OTM-33A	EPA “other test method” 33-A.
Pa	Pascal. Measure of pressure. One atmosphere of pressure is equivalent to 101,325 Pa.
plume	Mixture of gas and air, moving downwind from an emission source.
POD	Probability of Detection.
ppm	Parts per million. Measure of concentration.
PVC	polyvinyl chloride, a common building material.
PVC	Polyvinyl chloride.
Ro	MOS resistance for clean air.
Rs	Measured MOS resistance.
Screening Period	Time required for all equipment locations of a site to be sampled by the network of BluBird nodes

Term	Definition
shop	The warehouse where BluBirds are built and tested.
SSL	Secure sockets layer (data transfer protocol).
TDLAS	Tunable Diode Laser Absorption Spectroscopy. A technique for measuring the concentration of certain species such as methane.
V	Volts.
VOC	Volatile Organic Compound (typically referring to non-methane VOC).
VPC	Amazon Virtual Private Cloud.

Table 1: *Description of terms and methods as used in Description of Technology Document*

1.2 High Level Workflow

Figure 1 provides a high-level overview of the workflow of the BluBird technology, which includes the following steps:

1. BluBird device samples ambient air
2. Encrypted data sent to cloud software
3. Security and routing
4. MOS reading converted to methane concentration (see Figure 2)
5. Methane concentration converted to emissions rate (see Figure 3)
6. Emissions rate during periodic screening period is calculated
7. Client notified
8. Verification

Additional details on the steps to convert the sensor readings to a methane concentration are provided in Figure 2. Similarly, additional details on the steps to convert the methane concentration to a mass emission rate are provided in Figure 3. Figure 4 provides the security cloud architecture workflow.

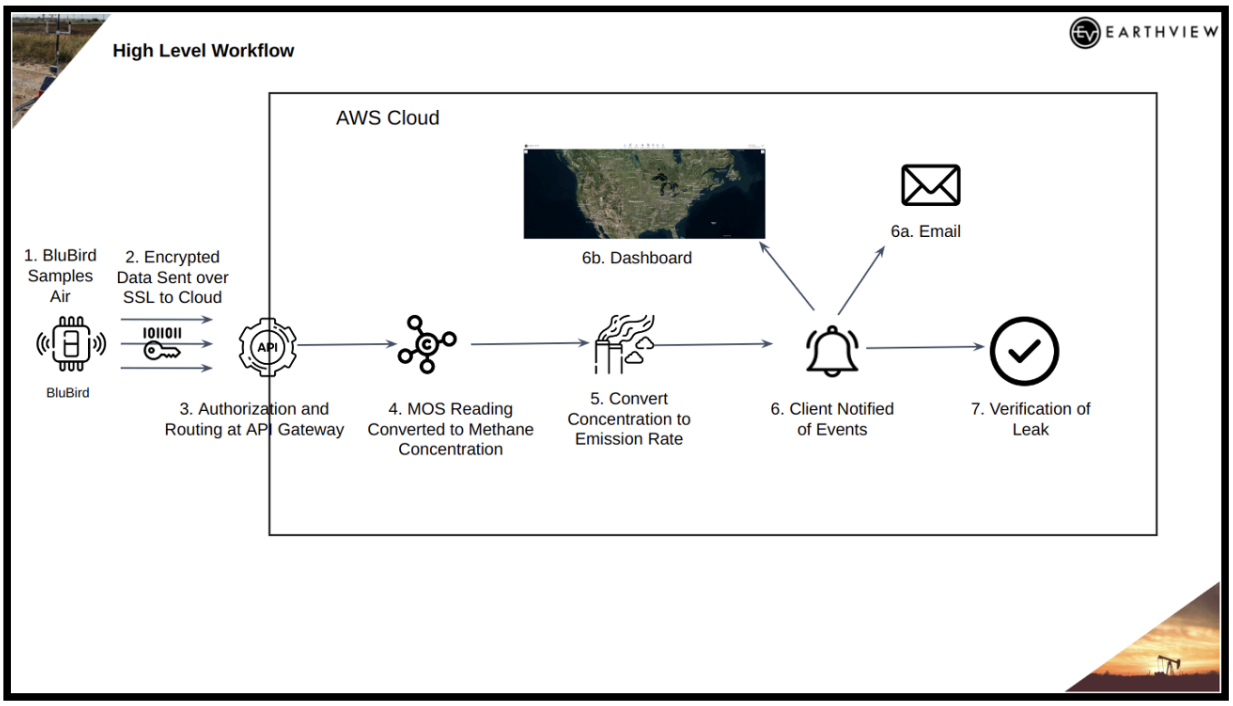

Figure 1*: High level workflow of the BluBird CMS system.*

[Confidential Business Information Redacted]

Figure 2: *Flow chart of MOS reading to methane concentration*

[Confidential Business Information Redacted]

Figure 3: *High level workflow of Methane Concentration to Emission Rate*

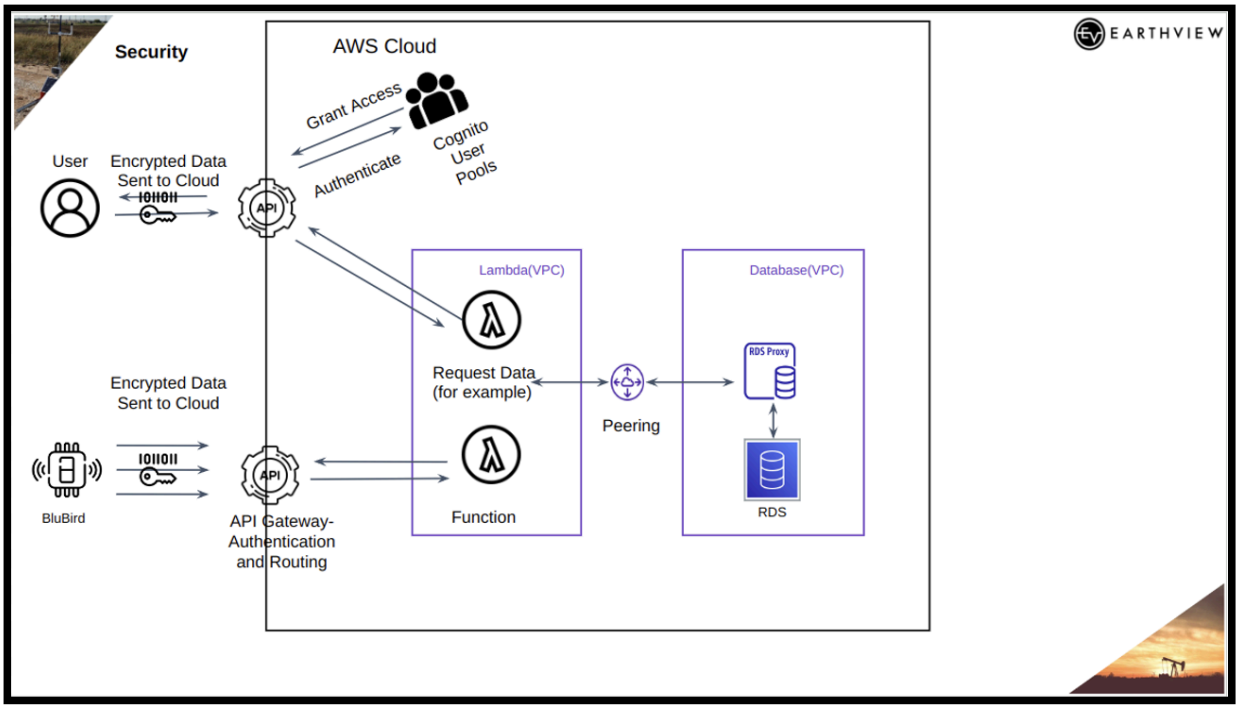

Figure 4: *High level security cloud architecture.*

2 Description of Candidate Measurement Technology

The BluBird gas monitoring system is a patented and patent-pending combination of sensing hardware and analysis software.[1] It consists of the measuring and reporting instrument (the BluBird itself), the cloud-based computations that convert measurements into methane and VOC concentrations and then converts these concentrations into estimated emission rates, and the cloud-based tools and human interactions that deliver the information to the customer. Emissions are monitored continuously, with data processing applied that is consistent with the requirements for period screening. In this document, we refer to the field instrument portion of this system as the BluBird, and the cloud-based software as the Gridded Pad Analysis and Quantification System (GPAQS). The "BluBird CMS" refers to the entire system - field sensors, firmware, cloud-based software, and cloud-based data dashboard. A basic part of the

[1] U.S. patent Application # 17/735,436, “Gas Leak Detection System”, approved 6/10/24; see US_20220357232_A1_I_approved_patent.pdf in Supplemental Materials.

processing software is an Earthview-developed “digital twin” (Glaessgen and Stargel, 2012; IBM, 2024) of the MOS sensors - essentially, virtual models of the sensors - that allow Earthview to estimate how various factors affect the MOS measurements using real-time data.

2.1 Company Background

Earthview headquarters is located at 908 Dragon St, Dallas TX 75207. Earthview Corp. is incorporated in the U.S. as a C corporation.

Earthview is the provider of the measurement system using advanced methane detection technology.

Earthview products are readily available, and are leased, licensed and offered for sale.

Earthview has been monitoring the oil and gas sector domestically since 2019.

The proposed ATM is being proposed as a periodic screening technology. It is broadly applicable across the oil and gas sector. Earthview systems are currently operating at 120 oil and gas production sites, with a total of 480 sensor units deployed in the following basins:

- Permian
- Eagle Ford
- Marcellus
- Barnett
- Haynesville

2.2 Scientific Theory

2.2.1 Hardware Design

The BluBird hardware design is based on well-documented theory regarding gas sensing and methods for converting sensor data to methane concentrations (see Section 1, Section 2.2.2 and elsewhere in the application for supporting references):

- Target gases of interest (methane and heavier VOCs) are known to react with MOS.
- Individual versions of MOS have different response levels to different gas types
- These reactions occur at gas levels sufficient for monitoring applications.

- These reactions are measurable as changes in voltage at response levels sufficient for electronic processing.
- The resulting measurement signals can be stored onboard and transmitted to a host computing center.
- The measurement process is repeatable and sustainable at a rate of at least once per minute.
- Operation of all system functions can be sustained over time, using solar power.
- Machine learning methods can separate gas-induced signals from sensor changes and environmental influences.
- It is possible to develop sensor response functions that relate resistance to gas concentrations.
- These sensor response functions are sufficiently stable over time and between instruments.
- The full system is cost effective and suitable for large-scale deployment.

The basic theory of operation for the BluBird field instrument is to allow an air sample to interact with a set of three MOS sensors and with air temperature and humidity sensors to generate electronic signals correlated with methane concentration, VOC concentration, air temperature and air humidity. The theory behind the use of this set of sensors is based on known MOS sensor operations theory and known performance characteristics.

Multiple MOS sensors are used to provide the necessary data for subsequent application of signal processing methods to extract methane and VOC concentrations and to infer the effects of changes in humidity and temperature (e.g., Wang et al., 2010; Abdullah et al., 2022; Robianni et al. 2023). Earthview recognized from early testing that the amount of heavier VOCs (ethane, propane, and butane in particular) affects the conversion of MOS readings to methane concentration. To help address this as well as to provide other useful information about emission sources, a set of three MOS sensors are used. Each MOS exhibits different sensitivities to methane and VOC while also having different responses to humidity and air temperature. Fusion of these data allows us to infer VOC content. Based on this knowledge (as well as any information on natural gas composition that the operators can provide to us), we select the sensor-to-concentration conversion response function most appropriate for the situation. Unlike the MOS sensor, the air temperature and humidity sensors are essentially unaffected by trace natural gas amounts, so therefore provide an independent measure of temperature and humidity.

It is worth noting that our inclusion of a MOS sensor that responds to non-methane VOCs has advantages over methane sensing alone. Knowledge that an emission contains a substantial amount of heavier VOCs is useful for determining the most likely leak source (for example, a leak from a storage tank is more likely to contain VOCs than a leak from a wellhead). Also,

non-cooled OGI cameras and TDLAS tuned to detect methane may miss the presence of VOCs, so could potentially fail to detect leaks that consist mainly of heavier VOCs.

2.2.2 MOS Sensors

2.2.2.1 Basis of Operation

MOS sensors, initially developed in the 1960's (Seiyama et al., 1962) measure gas presence by detecting changes in electrical resistance when exposed to target gases (Prabakaran et al., 2015; Isaac et al., 2022; [see also Section 1]). The basic measurement is the change in resistance across a sensing plate caused by the target gas (e.g., Aldafeeri et al., 2020). Using thick film manufacturing techniques, a sensing material consisting of a metal oxide semiconductor is coated onto electrodes made of a noble metal, which are printed onto an aluminum substrate. Tin oxide (SnO_2) is used for the MOS included in BluBird. Different metal oxides, such as SnO_2, ZnO, and TiO_2, have varying attraction preferences for different gases, which affects their sensitivity and selectivity.

The two electrodes are connected as positive and negative, with two additional power connections assigned to a heating element (RuO_2), that is printed on the reverse side of the sensing plate, and which heats the plate. The plate is typically heated to a range of 200-400°C. The MOS' response to a specific gas can vary with plate temperature, so it is important that the electronic circuitry provides a stable power supply at the recommended current.

As discussed in the next section, the sensitivity of metal oxide gas sensors is influenced by the chemical composition, surface modifications, microstructure, operating temperature, humidity, doping, and electrode configuration. These factors collectively determine the efficiency and effectiveness of the sensor in detecting specific gases.

The specific MOS sensors used in the BluBird have been shown to be capable of measuring methane concentrations at the low ppm level, albeit with calibration and adjustments for environmental effects (Eugster and Kling, 2012; Collier-Oxendale et al., 2018; Eugster et al., 2020; Riddick et al., 2020; Barchyn et al., 2023) and the TGS2611 (Bastviken et al., 2020; Shah et al., 2023).

For reference, Torres et al. (2022) include field-test results from a comparable metal-oxide based methane sensing system, which demonstrated the ability to detect methane concentrations of 0.5 to 1 ppm above background. This is consistent with our test results presented in Section 3.3.3.

2.2.2.2 Factors Affecting MOS Performance

MOS sensors are known to be highly sensitive with a rapid response time, but are affected by a variety of factors that can mask this sensitivity (Schutz et al., 2017; Abdullah et al., 2020). Our approach for addressing the effects of influencing factors are described in Sections 3.2.1 and 3.2.2. This approach is best thought of as a “digital twin”, or a virtual model of a physical object. Earthview builds such a twin individually for each individual MOS sensor using real-time measurements and derivatives of these measurements. The twin is then used to estimate how the individual MOS sensor is likely to react to measurements of the parameters influencing the sensor. In our approach, the digital twin is based on statistical relationships that model the effects of environmental conditions (humidity and to a lesser degree air temperature, primarily) on the MOS sensors’ response. The humidity effects modeling described by Yan et al. (2021) is a simpler example of this general approach.

Key influencing factors include the following.

Humidity:

As noted above, it is well known that an increase in moisture content in the air sample reduces the ability of a target gas to adsorb onto the MOS sensing substrate (Wang and Zhou, 2022), mainly by production of hydroxyl groups that are adsorbed onto the sensor element, leaving less space for reaction of the sensor with the target gas (e.g., Sohn et al., 2007; Vasiliev et al. 2018, Isaacs et al., 2022). Consistent with this, Abdullah et al. (2020) reported a decrease in sensitivity with rising humidity. In contrast, it has also been remarked that MOS sensor accuracy can decrease substantially at low humidity (Eugster and Kling, 2012; Riddick et al., 2020). However, consistent with the hydroxyl adsorption issue noted above, we find no apparent decrease in accuracy at low humidity. There is a change in sensor behavior at humidity very near 0% which, as noted by Riddick et al. (2020), complicates the use of calibration gas (which is at essentially 0% humidity). This can be addressed by adding some humidity using nafion tubing or a bubbler bottle, as is described in Maslanik (2023b; see WP-2023-11 in Supplemental Materials). Our tests using calibration gas treated in this way does not show any drop-off in performance of the sensors at low humidity.

This approach also allows us to create sensor-to-methane conversion equations that are applicable at low humidity and that can be applied to field-collected data. Combined with Earthview’s auto-calibration procedure that continually identifies clean-air resistances for each sensor unit, the result is no discernable decrease in sensor performance across a normal range of humidity. In fact, we can take advantage of higher sensitivity as humidity decreases. Furthermore, the approach we use for the BluBird sensor chamber and air flow appears to help reduce the sensitivity loss associated with high humidity (Sohn et al., 2007).

Cross-sensitivity to other gases:

While MOS sensors are engineered to respond most strongly to specific gases, they are affected by other gases that have similar interactions with the MOS sensing material (e.g., Dahl et al., 2021). Earthview addresses this by choosing sensors that are less likely to show cross sensitivity, by using a set of three different MOS that each have different cross-sensitivity characteristics, by including a filter-equipped sensor, by testing the effects of different gas combinations, by calculating VOC concentrations in addition to methane concentrations, and by choosing sensor response functions (equations to convert from sensor measurements to methane concentrations) that help account for gas mixtures.

Sensor Drift:

MOS sensors are long-lasting and resistant to contamination. However, exposure to certain gases or contaminants can permanently alter the sensor surface, reducing its sensitivity. These include substances containing silicone (which can be found in some lubricants, desiccants, and hydraulic fluids, for example), and prolonged exposure to high concentrations of sulfur-containing gases, including hydrogen sulfide and sulfur dioxide. MOS sensors tend to experience drift in their baseline resistance over a long period of operation, which can affect their sensitivity (Isaacs et al., 2022). This drift is often caused by aging of the sensor materials. However, they are generally considered to be stable over 2 to 3 years (Dhall et al., 2022), and have a longer lifetime than other gas sensor technologies (Chai et al., 2023). Consistent with this, manufacturer's data for the MOS sensors used in BluBird indicate that they are quite stable over time. Romain and Nicolas (2010) found a significant drift, albeit over a period of multiple years, and using ethanol as the test gas, which may have accentuated the drift compared to stability with methane. Even so, Romain and Nicolas (2010) outline a method to address drift. This method is essentially encompassed in Earthview's data processing approach. Van den Bossche (2017) tested one of the types of MOS sensors used in BluBird over 31 days and found no significant change in performance over that time.

We are also able to investigate whether our BluBird units show any indication of sensor response changes. The time series of resistances for the a year-long time series of BluBird measurements at a customer's well pad site (Figure 6) show no significant trends. Other measures, such as the rate of change of resistance with change in humidity, are also stable.

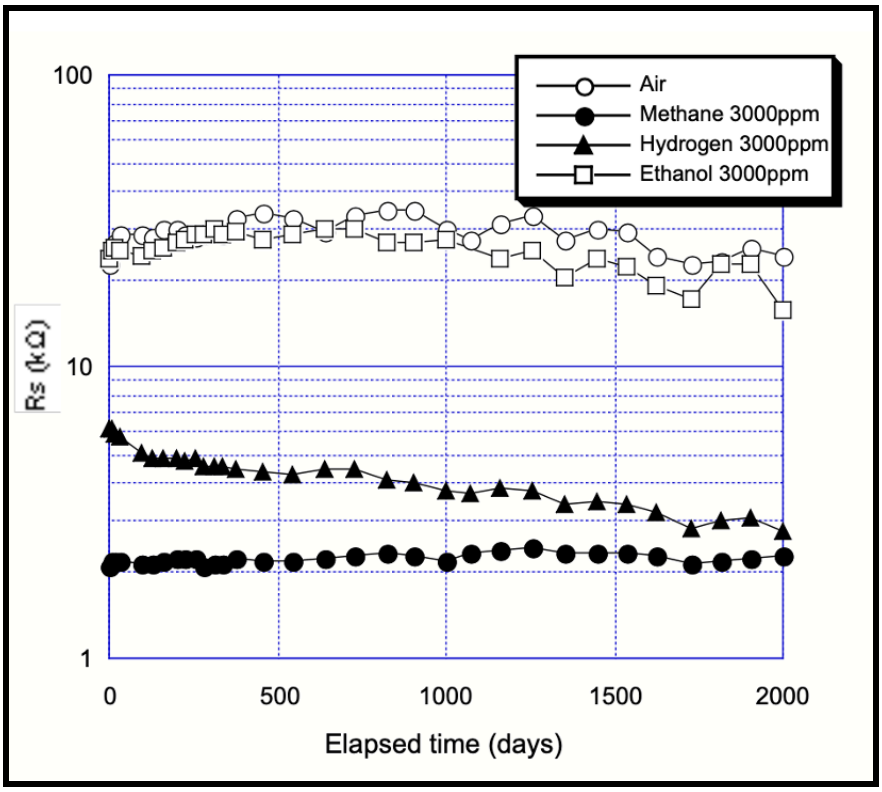

Figure 5. *Long-term stability of the MOS sensor 3 under continuous operation (from manufacturer's data sheet). The y-axis shows sensor resistance. The test was done using constant exposure to 5000 ppm of methane, 3000 ppm of hydrogen, and 3000 ppm of ethanol.*

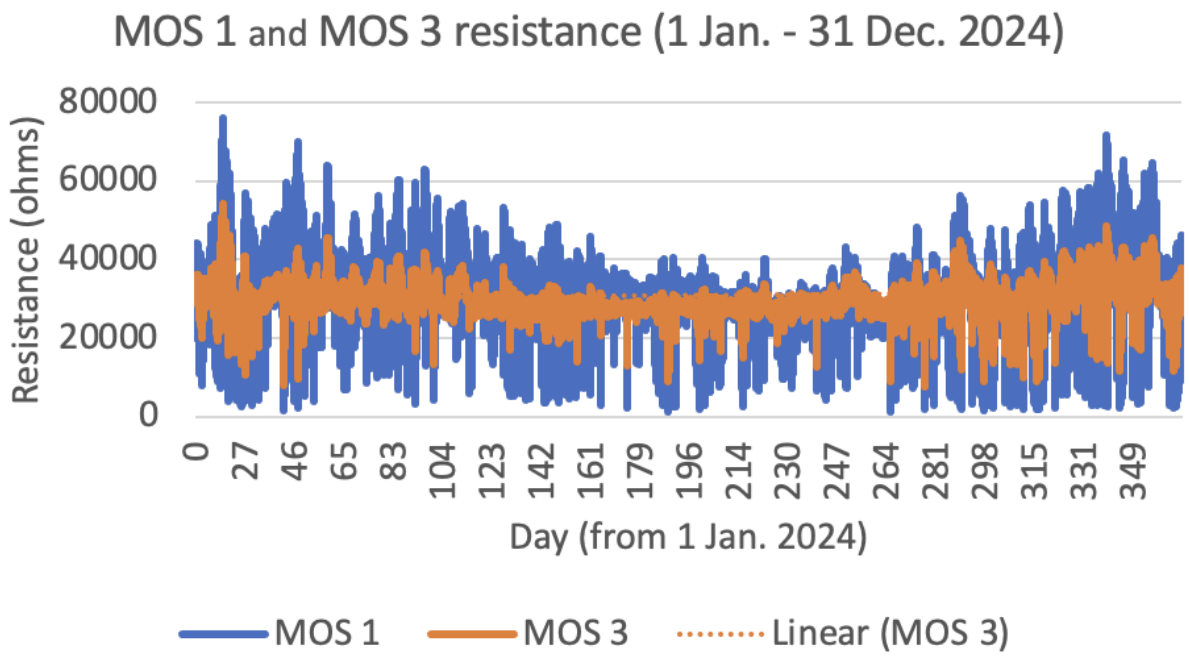

Figure 6. *Time series of TGS2600 (MOS 1) and TGS2611 (MOS 3) resistances for a BluBird node spanning the period from 1 Jan. through 31 Dec. 2024. The data show no significant drift in sensor readings over the 1-year period.*

Poisoning:

MOS sensors are long-lasting and resistant to contamination. However, exposure to high concentrations of certain gases or contaminants can permanently alter the sensor surface, reducing its sensitivity. These include substances containing silicone (which can be found in some lubricants, desiccants, and hydraulic fluids, for example), and prolonged exposure to high concentrations of sulfur-containing gases, including hydrogen sulfide and sulfur dioxide.

Environmental Effects:

Prolonged exposure to high temperatures, humidity, and other environmental conditions can degrade the sensing material over time.

Lifespan:

MOS sensors typically have a useful lifespan of around at least 2 to 3 years, after which their sensitivity and repeatability may decline (e.g., Chai et al., 2020). Earthview's standard operations plan is to retrieve and refurbish or replace nodes before this occurs.

Surface Changes:

The sensing layer's surface area and microstructure can change over time due to thermal cycling and gas exposure, affecting sensitivity. Earthview has developed a means of detecting changes in sensitivity, which we use to track changes over time.

To mitigate these issues, approaches such as the following can be used:

- Regular calibration and baseline correction to compensate for drift.
- Sensor response modeling (see the discussion in the next section regarding methods used by Earthview).
- Maintaining a correct and stable MOS heating plate temperature. BluBird's circuitry is custom designed to help maintain constant and known current flow to the MOS.
- Periodic heating of the sensor to above normal heating-plate temperatures to help remove accumulated impurities (this is not available with BluBird v. 2 but is planned for BluBird v. 3).
- Modular design that allows for easy replacement of sensors. The MOS are replaceable in BluBird v.2.
- Earthview uses signal processing and machine learning techniques to identify and compensate for aging effects (see Section 2.2.5).

2.2.2.3 Consistency Between Figaro Sensors

The consistency between individual types of MOS sensors plays a role in how to convert from resistances to gas concentrations. We find that the resistance values can differ considerably between individual MOS sensors of the same type. However, using the ratio of the observed resistance to the predicted clean air resistance (Rs/Ro) (Eugster and Kling, 2012; Riddick et al., 2020; Figaro USA, 2021) helps normalize this variability. This ratioing effectively cancels out the bias introduced by the differences in individual sensors and helps to address shortcomings of MOS cited by Riddick et al. (2020; 2022). For instance, if the predicted resistance is calibrated for each individual sensor, then the ratio (Rs/Ro) will remove the sensor-specific bias. This approach is fundamental to the response functions developed by Earthview for calculating gas concentration accurately.

In simpler terms, even though the resistance sensitivity can differ between sensors, using the ratio of observed resistance to the trained, predicted clean air resistance ensures that any sensor-specific biases are minimized. This makes our calculations of gas concentration more reliable and consistent without the need for manual calibration.

2.2.2.4 Methods to Mitigate MOS Performance Degradation

2.2.2.4.1 Sensor Modeling in Lieu of Calibration

A traditional calibration approach requires exposing a sensor to known concentrations of a target gas. For methane monitoring using MOS sensors, this would require not only exposure to one or two known concentrations (i.e., a single-point or a two-point calibration), but to a range of concentrations. This is necessary since the MOS response function to gases is non-linear except over a limited range of concentrations. Furthermore, this multi-point calibration would need to be done over a range of humidity and temperature conditions since the resistance reading for a given gas concentration will vary with humidity and temperature. It is easy to imagine how such calibration becomes highly impractical in the field; particularly when there may be thousands of instruments to visit. Single- or two-point calibrations done under a single set of atmospheric conditions could still identify changes in sensor performance, and so have some value, but they still leave some room for uncertainty, including not really knowing how the system is behaving in-between calibration visits. There is also the issue that, depending on how the MOS resistances are converted to methane concentration, it may be necessary to carry out a calibration of most if not all instruments prior to deployment so that it is possible to compensate for deviations in sensor responses over time.

Early on, Earthview concluded that the above type of calibration would be unsuitable for our goal of deploying thousands of sensors capable of providing consistent and reasonably accurate gas measurements under highly variable field conditions. We therefore developed an alternative approach to address sensor performance and drift issues by (1) calculating expected resistances given measured atmospheric conditions and (2) determining observations that represent likely “clean-air” background conditions. This approach, presented in Earthview patent US_20220357232_A1_I, is based on the idea of a virtual model of the sensors, referred to as a “digital twin” (Glaessgen and Starget, 2012; IBM, 2024). The model, which is constructed using machine learning methods applied to the time history of data at each BluBird location, calculates the expected sensor resistance under observed environmental conditions but with assumed background “clean air” concentrations of methane, thereby compensating for atmospheric effects and sensor changes. The differences between the modeled clean-air resistances and the observed resistances are used to estimate methane concentration. Earthview builds such a twin individually for each deployed MOS sensor using real-time data, with the twin model allowed to evolve over time.

2.2.3 Plume Dispersion Modeling Theory

The proposed ATM assumes that emissions from a source will be transported from the source to the sensor via wind transport and/or lateral diffusion. When weather conditions are appropriate,

Earthview uses an inverse version of the standard Gaussian plume model to calculate methane leak rates (alternate models are used in other conditions, as discussed below). This is a widely used approach (e.g., Turner, 1970; U.S. EPA, 2014; Foster-Wittig et al., 2015; Caulton et al., 2018), with a long history. Lotrecchiano et al. (2020) provides an easy-to-follow overview of its advantages and disadvantages for real-time applications. The applicable theory is that knowledge of local atmospheric conditions (winds, surface-layer stability, turbulent mixing potential, etc.) along with knowledge of relative positions of sensor and emission source, can be used to predict the degree of dispersion of methane along its travel path from source to sensor.

Details of our implementation are presented in Section 4. In cases for which Gaussian plume model assumptions are questionable (such as for low-wind or calm conditions, and for very short distances, we employ alternative models as discussed in Section 4.1). Our modeling implementation follows the methodology outlined in EPA's Other Test Method (OTM) 33A and applied to oil and gas pad sampling (U.S. EPA, 2014; Robertson et al., 2017; Edie et al., 2020).

When doing OTM-33A sampling, the measurement instrument is maneuvered to try to position it within the centerline of the emissions plume, where concentrations are expected to be greatest, based on the Gaussian distribution. Fixed continuous monitoring sensors such as the BluBird instead rely on variations in wind direction to approximate this. (An example of testing the mobile version of the original sensor prototype is given in Maslanik et al., 2021 [see WP-2014-1 in Supplemental Materials]). The remaining difference is that, unlike the OTM-33A sensor package, height between the fixed sensor and the plume's maximum concentration zone cannot be adjusted.

2.2.4 Practical Considerations for an Effective GMS

The basic idea that underpins the BluBird continuous monitoring system (CMS) is that inexpensive sensors, when combined with sophisticated processing and supporting data, can provide effective emissions monitoring in a practical way. By "effective and practical", we mean:

- capable of detecting and quantifying emissions at relevant, actionable levels
- capable of delivering this information to the operators in a timely manner (within one hour of detection based on emission rates, or within 10 minutes based on high concentration readings)
- able to function in the field for long periods with minimal or no maintenance
- imposes minimal burden on operators in terms of installation and interference with site operations.
- inexpensive enough that operators can afford the system, with positive benefit vs. cost considerations
- deployable at hundreds to thousands of locations

We can expand on some of these aspects:

- "relevant" and "actionable" levels of emission detection are levels that are clearly above site background levels during normal operation, and that are presentable in ways that allow the operator to immediately see the potential severity of the leak
- accurate measurements of gas concentration requires that the CMS be able to handle a wide range of weather conditions. In the BluBird's case, due to its dependence on MOS sensors, this goes beyond just surviving such conditions (which of course is still critical), but also the ability to account for the effects of changing conditions on the MOS readings themselves
- since we intend the BluBird CMS to be a cost-effective solution that can be deployed at thousands of locations, its accuracy must not depend on frequent visits for instrument calibration
- from our experience with customers, a practical CMS solution is one that alerts them quickly to an on-site leak so that they can respond to it promptly. In many cases, this results in an immediate repair
- a practical solution is one that is inexpensive but yet effective enough to allow the operator to justify the cost based on its own merits, without necessarily needing to be driven by regulations.

Work by Eugster and Kling (2012), Maslanik (2014), Collier-Oxandale et al. (2018), Riddick et al. (2020; 2023) and others have shown that inexpensive MOS sensors have the potential to monitor methane emissions in the field, but with some shortcomings. Earthview has substantially addressed each of the factors limiting the performance or practicality of MOS sensing for methane detection.

2.2.5 Number of Devices, Device Placement and Site Setup

Fenceline monitoring systems are influenced significantly by wind speed (through plume transport and dispersion), wind direction (which dictates path of travel between source and sensor), the size of the pad, and the location of oil and gas production equipment. To optimize these factors, Earthview uses an algorithm to determine the optimal number and placement of devices at a location.

When Earthview plans a site installation, the first step is gathering wind data from the nearest weather station. The latitude and longitude of the target site are used to identify the closest weather station. Once identified, the previous year's wind data from the station is retrieved and organized into a wind rose graph (Figure 7). This data is sourced from publicly available records from the Iowa Environmental Mesonet.

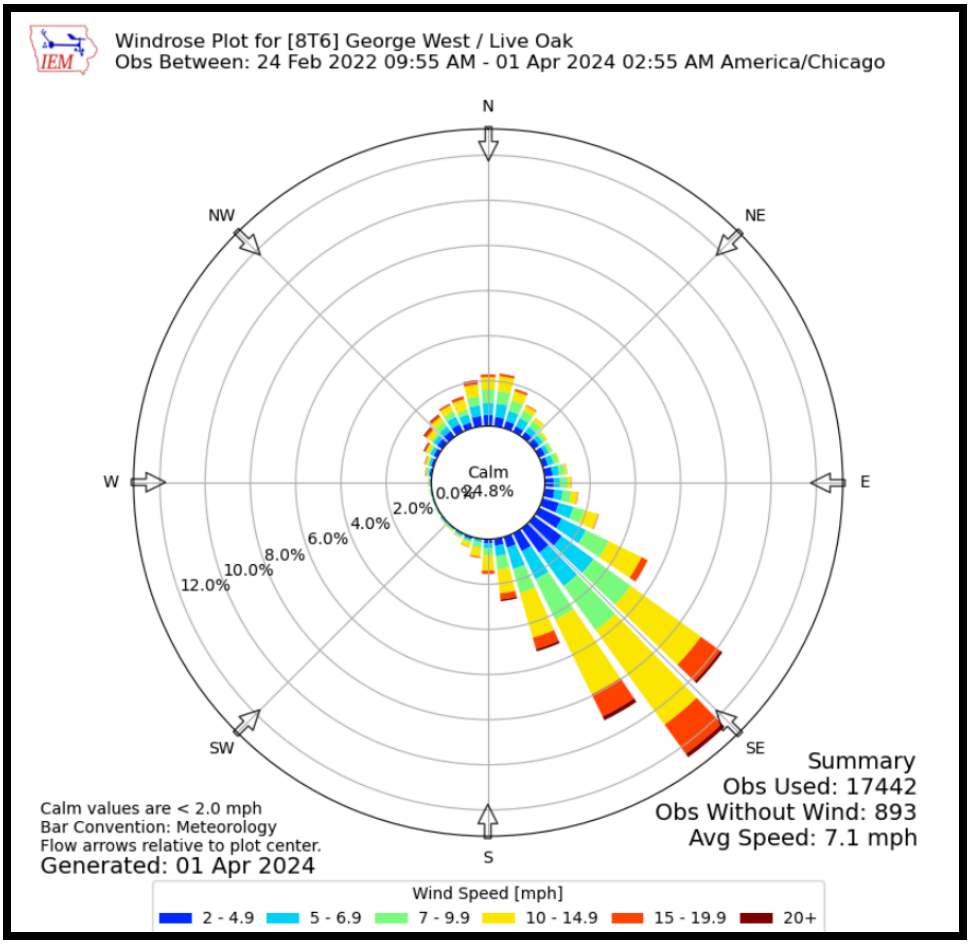

Figure 7. *Wind rose data example (from Iowa Environmental Mesonet).*

As a reminder, winds are labeled based on their origin. Referring to Figure 7, this means the winds predominantly originate from the southeast. For continuous monitoring to be most effective, devices should be placed downwind from production equipment. In the example shown in Figure 7, this would mean placing the devices predominantly in the northwest, downwind from the production equipment.

In practice there is typically significant variation in wind direction across an entire year or even day-to-day. To best account for this variability, Earthview has found success in using an algorithm that is confidential business information and redacted.

2.2.6 Site Coverage and Number of Nodes

The number of sensor nodes deployed is based on the complexity of the site, degree of variation in wind direction, desired time to achieve complete sampling coverage, and emission quantification accuracy needed. As noted in Section 4.2.2 ("Grid Layout") and Section 4.3 ("Emission Action-Level Analysis for Periodic Screening"), for periodic screening as defined in CFR §60.5397b(c), the number and placement of nodes is dictated by (1) the need to provide detection capability consistent with previous testing, and (2) the time required to obtain full site coverage during a periodic survey based on variations in wind direction. As discussed in Section 4.3, for periodic screening applications, the number and positioning of BluBird nodes should be arranged such that all potential emission sources are less than approximately 100m from a node. This is recommended so that expected system performance for probability of detection is consistent with testing data.

For each pad, the Earthview system can calculate how much time was required to observe (i.e., have an alignment of wind blowing from a source to a BluBird) some or all of the potential sources on the site. On average, 100% of the source locations for a subsample of sites were observed within a time span of about 3 to 6 hours. Therefore, it can be expected that a periodic screening survey will typically require approximately 6 hours. Since Earthview's GPAQS system can automatically determine when 100% of a site has been sampled, the actual survey time for a periodic screening event can be allowed to vary from site to site.

[Confidential Business Information Redacted]

2.3 Description of Physical Instrument

2.3.1 Introduction

Designed and manufactured by Earthview specifically for monitoring oil and gas production and processing facilities, the BluBird point sensors are low-cost, solar-powered instruments that are easy to install, portable, and require no site modifications or extra infrastructure. The field units are rugged and reliable, with no routine servicing needed. This makes them well suited for remote, hard-to-reach locations. Any number of sensors - from one to hundreds - can be deployed at individual sites.

The basic technology uses an array of metal oxide semiconductor (MOS) gas sensors, regulated air flow via a pump, an adjustable-height mast with air intake, solar power and backup battery, in-situ wind and environment sensors to continuously monitor changes in trace gas concentrations and local conditions that affect gas dispersion and mixing. See Figure 10 for an overview of a standard Earthview BluBird in the field.

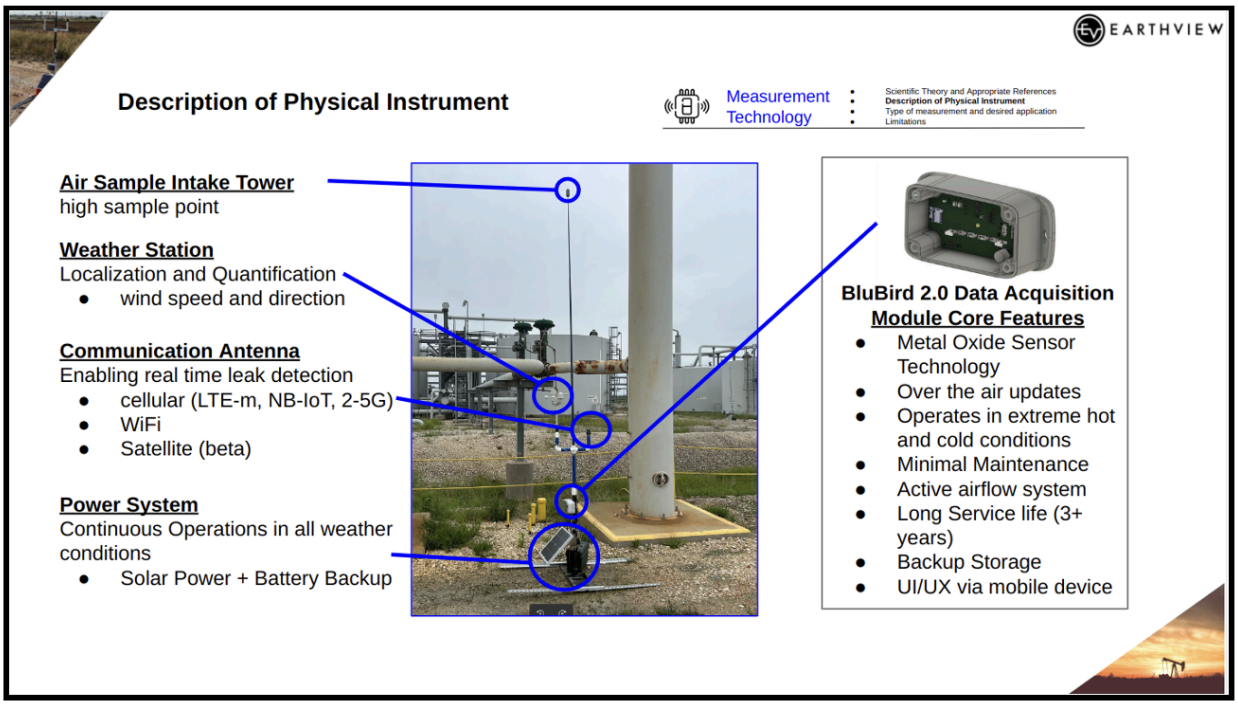

Figure 10. *Earthview BluBird sensor. Consists of a folding stand, solar panel, backup battery, instrument case, cellular antenna, wind sensors, and adjustable mast with air intake.*

2.3.2 External Components

2.3.2.1 Air Sample Intake Tower

The BluBird mechanical design utilizes PVC as the main building material as it is low weight, low cost and available around the country. Both SCH40 and SCH80 PVC are used according to mechanical strength requirements. The sample intake tower is made of PVC material with an adjustable telescoping pole to optimize the ideal sampling point of the theoretical plume coming off production equipment. Typically this pole is set between 15-20 ft. but can be adjusted further depending on customer needs. Since methane rises, it is

advantageous to have a higher sampling point so that the plume does not pass above the top of the sample intake tower. Assuming wind speeds greater than 1 m/s, it has been found that there is generally enough plume dispersion in the vertical plane that a sampling height of about 20 ft. is adequate to sample emissions off tall pieces of production equipment, up to 30 ft.

The air intake subsystem's theory of operation is that a sufficient air sample, free of liquid water and other material, can be extracted from the ambient air and transmitted into the BluBird sensor chamber while remaining essentially uncontaminated during its passage. The air intake subsystem achieves this using a custom-designed intake mounted onto an adjustable-height mast. Teflon tubing extends from the intake, through the inside of the mast, into a connection on the BluBird enclosure. A water trap is included to capture liquid water before entering the enclosure. Inside the enclosure, tubing connects the external intake to one end of the sealed sensor chamber. Tubing attached to the other end of the sensor chamber is connected to an air pump. This air pump draws a partial vacuum, pulling the air sample into the sensor chamber. For each sampling period, the pump runs through a set of pump cycles spaced over a period of multiple seconds. This variation in pump cycling was found to maximize the sensitivity of the MOS sensor responses.

2.3.2.2 Weather Station

Wind speed and wind direction are measured and reported by each BluBird device on a site. Earthview has concluded that, given the importance of wind patterns on gas dispersion, we can achieve better results in most instances by measuring winds at multiple locations. To keep costs reasonable, this typically requires that we use lower-cost wind cup and vane systems rather than more-expensive sonic anemometers. For special cases, such as where wind speeds are constantly very low, the potential also exists to interface with sonic anemometers that provide a voltage output for speed and direction. The main shortcoming of these instruments used is responsiveness at very low wind speeds.

2.3.2.3 Communication Antenna

The BluBird has a communications antenna that has both cellular and wifi capabilities. Devices will typically connect to the internet via cellular because most sites will not have wifi that is available to third party vendors. Many sites that are monitored are in low cell reception areas, so the data payload sizes have been minimized to the lowest byte size possible. There is also a caching mechanism in place where, if a device takes a sample and cannot send the sample to the server immediately, the device will cache the sample on a local SD card to send when the device is able to get an adequate cell reception. See a picture of the Earthview Communication Antenna in Figure 11.

Figure 11*. Communication Antenna. Sends local measurements to Earthview cloud servers.*

2.3.2.4 Power System

The BluBird power system consists of a solar panel and backup battery supply. The 12V battery is charged during the day when there is enough sunlight exposure to provide an adequate charge to the battery. This solar panel and backup battery provides a perfect balance of self sustaining power and fail safe backups. This power system is shown in Figure 12.

Figure 12*: BluBird power supply system: solar panel and backup battery.*

In a scenario where the battery voltage drops below 10V, the system drops into an under-voltage lockout mode to protect itself from draining the battery. While in this lockout mode, the BluBird will not take samples as there is not enough power to get appropriate

readings from the data acquisition module. As the sun comes back the battery will recover and when the voltage reaches 11V the device will wake itself up and continue sampling as normal. This under voltage lockout mode is not a frequent occurrence. The devices can operate for about 7 days without needing a solar charge, and almost any location will have sun at least one day with adequate UV exposure in a 7 day period. Figure 13 displays a healthy battery voltage pattern.

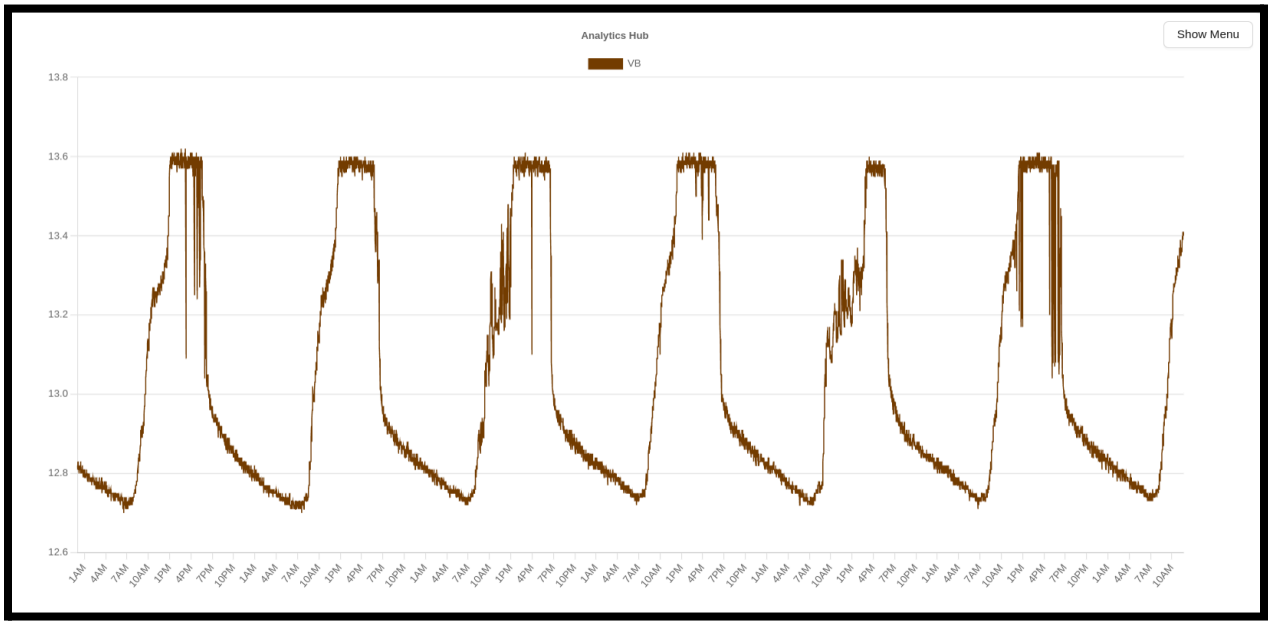

Figure 13*: A typical healthy battery voltage over a seven day period. Battery voltage quickly increases to full between sunrise and around 10AM. Battery voltage plateaus during the day at around 13.6 V. Battery voltage slowly discharges at night after sunset before repeating the cycle at sunrise.*

2.3.2.5 Power Conditioning

The theory of operation for the power subsystem dictates that a very high level of voltage and current stability must be maintained to achieve the best performance possible from the MOS. Doing so helps keep the MOS heating element at the optimal temperature appropriate for the sensing chemistry, and also avoids introducing spurious noise into the analog voltage output. All of the printed circuit boards used in the BluBird are custom designed for Earthview. This allows us to use state-of-the-technology circuitry design and printed circuit board construction, with no compromises. The result is an optimized design which would not be possible using off-the-shelf, general purpose, commercial board-based modules.

To keep the power subsystem with a high level of voltage and current stability there is a 5V rail that is often referred to as Figaro Voltage or Figaro V. The voltage capability of the system will

vary as the battery on the power system drains. This 5V rail is used to ensure as close to 5V as possible to send to the Figaro Sensors. Van den Bossche et al. (2016) noted that providing stable power is one way of improving the performance of the MOS sensors (specifically, the TGS2611).

2.3.2.6 Moveable Stand

The Earthview BluBird continuous monitoring system is mounted on a lightweight, “H” bracket stand (Figure 14). Field-operations engineers weigh down the stand with sandbags to prevent the system from blowing over or moving in a high wind environment. (BluBirds have successfully withstood winds over 50 miles/hr).

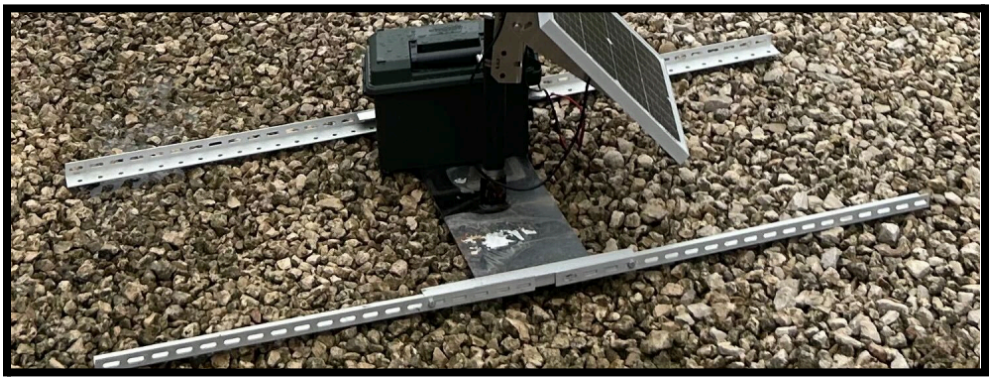

Figure 14*: Moveable support base.*

2.3.3 Data Acquisition Module

The data acquisition subsystem encompasses the sensors that measure air samples. It consists of three MOS sensors, partnered with air temperature and humidity sensors, enclosed in a sealed chamber. The theory behind this subsystem is that target gas in the air sample will interact with the MOS, generating changes in electrical properties that translate into measurable voltage signals (Section 2.1.2 MOS Sensors). The air temperature and humidity sensors are required for converting the MOS sensor signals into gas concentrations (see section 3.3.1 Response Functions for the theoretical basis behind application of the MOS and the conversion to gas concentrations). BluBird is designed so that the individual sensors can be replaced fairly easily if they show signs of degradation or have reached a point where the sensor response becomes unstable or not repeatable (typically 2 to 3 years) (Chai et al., 2022).

The data acquisition module of the BluBird is the most important piece of equipment to understand, in terms of how Earthview measures methane. Every 30 seconds, the pump pulls in an air sample from the top of the sampling mast. This air sample is passed through a chamber where MOS sensors perform measurements. The pump then purges the sample from the

system and the cell module sends the measurement data to the server. This process is depicted at a high level in Figure 15.

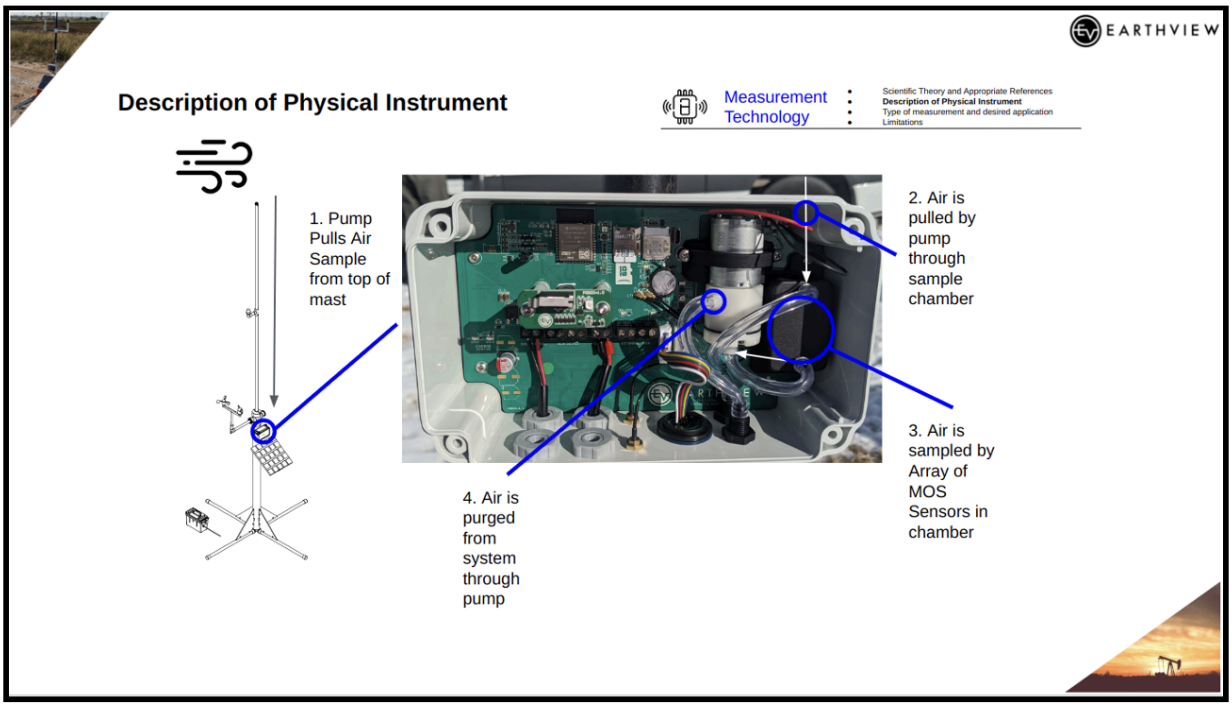

Figure 15*: BluBird air flow through system.*

2.3.3.1 Pump

BluBird uses a diaphragm-type pump (Figure 16) to pull air through the vacuum of the air sample control tower, through the MOS sensor chamber, and out through the pump. We have found that active air sampling using a pump is preferable to fans or passive air flow. It provides a more consistent sample, and is unaffected by wind speed or air movement direction. The air passes through the sensor chamber before the pump to avoid potentially introducing contaminants such as lubricants or plastic outgassing from the pump into the air sample. Life expectancy for a pump of this type is typically at least one year, based on reports of life spans of similar diaphragm pumps used for aquarium aeration. No pump failures have yet occurred in BluBird v. 2.0 systems, with some units having operated for over 12 months with no pump issues. For standard operations, the air pump is operated at 50% power, which increases pump life expectancy as well as reducing power consumption. Pump performance is tracked in real-time for all nodes using indicators such as current draw.

Figure 16*: Pump: pulls outside air into sample chamber.*

2.3.3.2 MOS Sensor Chamber

The MOS sensors are the core component of the BluBird methane monitoring capabilities. See section 2.1.2 MOS Sensors for a detailed discussion. The exact models and hardware design is confidential business information and has been redacted.

[Confidential Business Information Redacted]

2.3.3.3 Communications, time tagging, and positioning

The underlying driver of the communications, time tagging, and positioning subsystem is that all data collected must be readily transmitted to the Earthview cloud processing center, augmented with necessary information including sample time stamps and device position. This is achieved by using a cellular modem equipped with GPS, along with WiFi capability. A common modem IC is used that is capable of handling a variety of protocols, including non-U.S. providers. This IC includes a GPS which provides time and position independent of cell connectivity.

This subsystem also includes the cellular antenna. The BluBird installation provides different options for cellular antenna mounting positions as well as antenna type. These choices are made based on the quality of cell coverage at a particular site. When cell coverage is good, a lower-cost antenna is used, and is positioned lower on the BluBird's mount structure. When coverage is weak, a higher-performance antenna can be mounted at the top of the air intake mast.

Another critical element of this subsystem is the choice of cellular service provider. Earthview generally uses Hologram or T-Mobile for cell service. Satellite-based communications services are a consideration for future iterations of BluBird.

2.3.3.4 SD Card

A micro SD card is used to store data as a backup to the cellular/wifi data transmission. In situations where there is no cellular or wifi connection, measurement data is stored on the micro SD card. When wifi or cell coverage eventually returns, the data is then transmitted to ensure continuous sampling.

2.3.3.5 Air Temperature and Humidity Measurement

As discussed in Section 2.1.2.3 Factors Affecting MOS Performance, MOS sensors are highly affected by humidity, so an accurate measurement of humidity and temperature must be taken in order to correct for it in the conversion of MOS resistances to methane concentrations. These measurements must also be acquired quickly, with little sensor latency. To meet these requirements, the BluBird system uses the Renesas HS3001 sensor (see data sheet in Supplementary Materials) to provide air temperatures and humidity. The HS3001 is a highly accurate, fast-response, digital sensor with typical accuracies of +/- 1.5% for relative humidity and +/- 0.2 deg. C for air temperature. The sensor data are internally corrected and compensated to provide consistent accuracy over a large range of temperatures and humidities. User calibration is not required. To monitor overall conditions within the BluBird enclosure but outside of the sensor chamber itself, a Bosch BME680 sensor is used (see data sheet in Supplementary Materials).

2.3.4 Server Firmware Communications

The physical hardware is equipped with proprietary firmware that instructs the hardware how to function. The firmware has a plethora of functionality besides sampling for methane that aids in device health checks and ensuring a streamlined system.

2.3.4.1 Connection Flow.

Earthview uses encrypted Transport Layer Security (TLS) to communicate with devices in the field. This architecture is outlined in Figure 17.

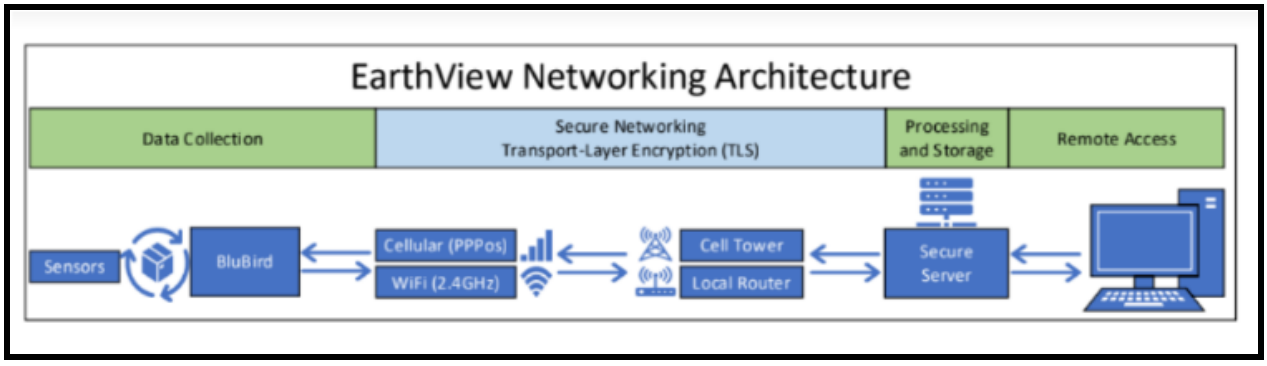

Figure 17. *Earthview networking architecture. Uses Secure Networking with Transport Layer Encryption.*

As mentioned, BluBirds communicate via cellular or WiFi protocols. The device initiates a connection to the Earthview server and engages in a handshake process to establish cryptographic keys to encrypt and decrypt data sent between the two parties. A description of HTTPS TLS Communication is provided below (Figure 18).

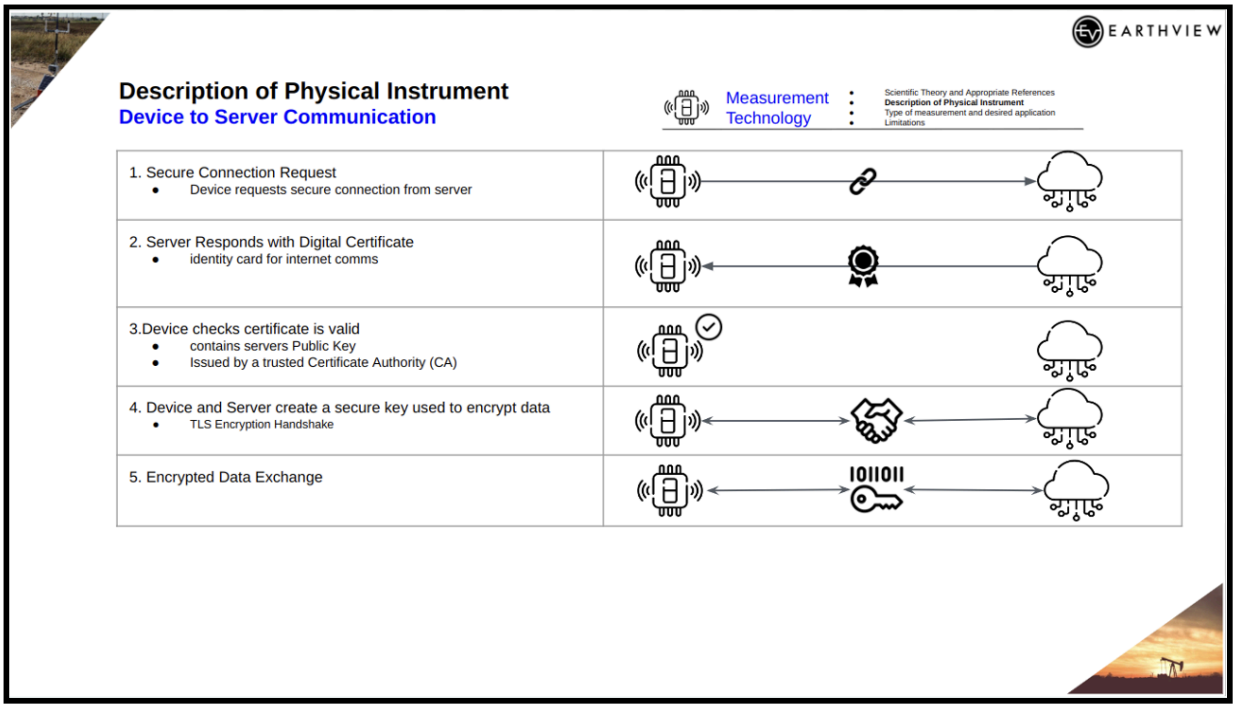

Figure 18. *HTTPS TLS communication with devices and Earthview servers.*

2.3.4.2 Reports

Before a device can be packaged and sent to the field, it must be tested and the measurements submitted to the server. This proves that all sensors are working as expected and prevents

issues that can occur from installing underperforming devices in the field. This initial test period also provides a baseline of sensor behavior that can then be used to assess changes in instrument performance over time.

The initial bench test of a device involves connection to the wifi hotspot of the device with a local device. Once logged into the device, the user can access the testing interface (Figure 19). After all tests pass, a report is sent to the server and the device is created in the Earthview database. Figure 19 has been redacted as confidential business information.

[Confidential Business Information Redacted]

After the initial bench test, the hardware to software communication is tested. To run the communication tests, an Earthview engineer will turn a device on and run sampling protocols that will send live reads to the server. The shop engineer will then use the Earthview dashboard to validate server device communication, which runs the tests listed in Table 3. A successful test screen is shown in Figure 20. Table 3 and Figure 20 were redacted as confidential business information.

[Confidential Business Information Redacted]

2.3.4.3 Over the Air (OTA) Updates

Earthview periodically releases new versions of the device firmware to units in the field. This can include security updates, performance optimizations, or new features. Since BluBirds are often in remote locations, it is unfeasible to have a field tech visit every BluBird to install these updates. Therefore, Earthview will typically update device firmware remotely.

Firmware updates are first tested on a single test device. Once that initial testing is completed, the firmware is then tested on a larger set of “beta” devices including some additional internal test devices and some devices installed in the field, where they can be closely monitored for failures. After a period of time without failure, the firmware will be approved and released to the entire fleet.

Every hour, BluBirds check in with the server to ensure they have the latest version of the firmware. If there is a new version, the devices will download and install it. After installation, the device will return to normal operating procedures and resume regular checks for new firmware versions. This process is outlined in Figure 21.

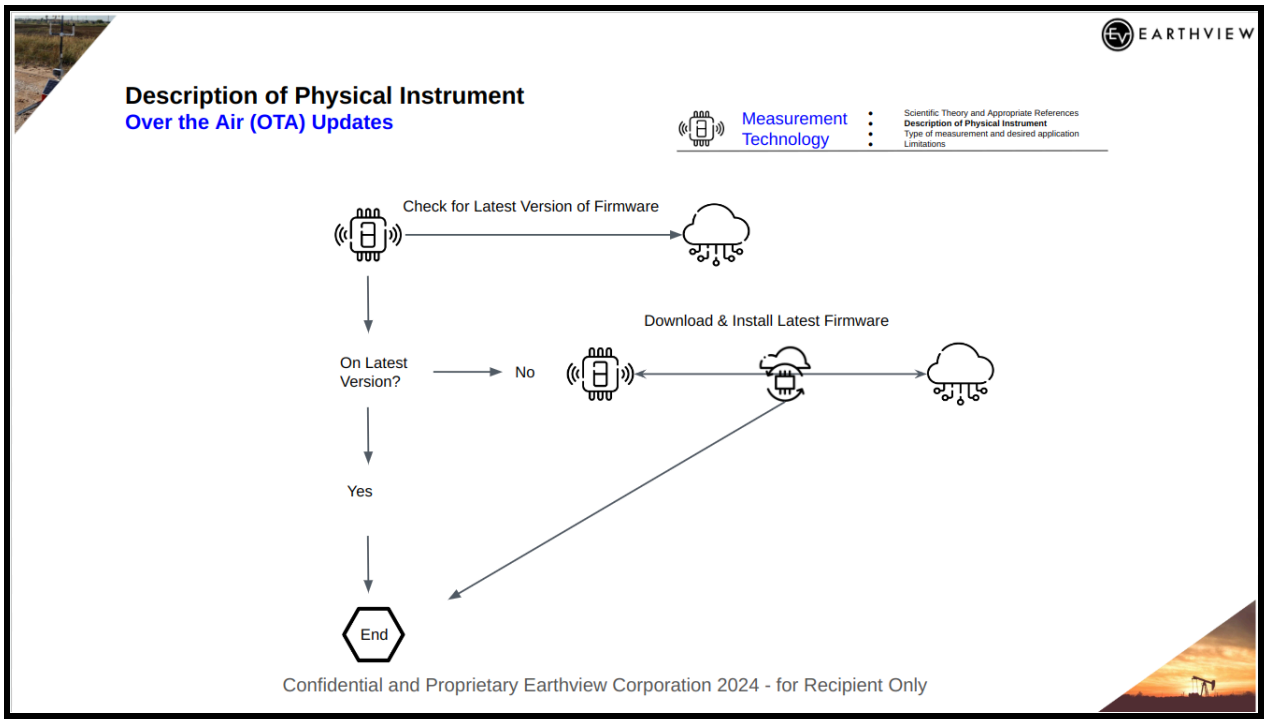

Figure 21. *Over the air (OTA) firmware updates workflow.*

2.3.4.4 Configuration

BluBirds can have their configuration updated in the field or remotely. These configuration settings include, but are not limited to, pump power, sampling frequency, Wi-Fi credentials or APN settings. If a field engineer modifies a device's configuration in the field, the BluBird will send its updated configuration to the server. Alternatively, engineers can update the device's configuration on the server and the device will update on the next hourly check-in.

2.3.4.5 GPS Location Check In

All BluBirds are equipped with GPS technology that will send a device's latitude and longitude coordinates every hour. When installed a field engineer will record the device’s latitude and longitude coordinates and send them to the server.

2.3.4.6 Sample Reporting

Measurement data from the BluBird are transmitted via the WiFi/Cellular network to the server for analysis. Table 5 lists these fields. Note Table 5 has been redacted as confidential business information. These fields are split into two groups that are measured at different frequencies: tier 1 and tier 2. Tier 1 fields have a higher sampling rate and are used for sensors that are critical for methane detection. Tier 2 fields are for relatively non-critical auxiliary measurements and are

sent less often than tier 1. The sampling frequency of tier 1 and tier 2 data is a configurable setting. Acceptable tier 1 and tier 2 frequency are listed in Table 4 below.

Tier 1	Tier 2
Continuous	1 minute
15 seconds	2 minutes
30 seconds	5 minutes
1 minute	10 minutes
2 minutes	15 minutes
5 minutes	20 minutes
10 minutes	30 minutes
	1 hour

Table 4. *Acceptable sampling frequencies for tier 1 and tier 2 sensor fields.*

[Confidential Business Information Redacted]

2.3.5 Monitoring Device Health (Status Checks)

Every twelve hours, the system automatically runs a series of health checks for all devices. These twice daily status checks help field operators be aware of necessary maintenance. Table 6 lists these status checks.

Status Check Name	Description
Online	Did the device send any data in the last 12 hours?
Connection	Is network signal quality above minimum acceptable threshold at least 80% of the time?
Validation	Did at least 80% of measurements pass validations?
Battery Voltage	Is the battery voltage at least 1V above 10V under voltage lockout threshold at least 80%

	of the time?
Battery Charging	Did the device's battery charge at least once in the last 12 hours?
Wind Speed Validation	Are at least 50% of wind speed measurements valid? *
Wind Direction Validation	Are at least 50% of wind direction measurements valid? *
Tier 1 Read Frequency	Did the device send at least 80% of the expected number of tier 1 reads?
Tier 2 Read Frequency	Did the device send at least 80% of the expected number of tier 2 reads?
Internal Humidity	Was the internal relative humidity measurement ever above 100%? **

Table 6. *Twice daily device status checks.*
** Local airport data is used in place of invalid wind measurements, so this check alerts operators to problematic wind instruments separately.*
*** Water-logged instruments can cause the humidity sensor to report erroneous 100%+ humidity values, a common occurrence in wet environments.*

To address the requirement that the network must operate with at least a 90% uptime, the online statistics discussed in Table 6 have been compiled since September of 2023 when these were first measured. This was determined on a rolling annual basis each month, meaning at the end of each calendar month, the downtime is calculated for the previous 12 months. Table 7 has statistics for each device and for each network. The network is defined as each site monitored, so that if at least one device on a site sent at least one read in a 12-hour block period that is considered a pass with the previous 365 days aggregated. The device column uses the definition that if a single device sent at least one read in a 12-hour block period that is considered a pass with the previous 365 days aggregated.

Date	(%) Uptime Per Site - Network
2024/07/01	99.36%
2024/06/01	99.46%

2024/05/01	99.35%
2024/04/01	99.29%
2024/03/01	99.66%
2024/02/01	99.71%
2024/01/01	99.56%
2023/12/01	99.14%
2023/11/01	98.70%
2023/10/01	97.73%
2023/09/01	94.81%

Table 7*. Annual uptime status checks per device and per site.*

2.4 Type of Measurement

The BluBird CMS is an in-situ continuous monitoring system that is deployed along the perimeter of an individual oil and natural gas facility (e.g., well-pad, compressor station, etc.). Earthview has current deployments of the BluBird CMS at (list all site types where installations currently exist) across the (list basins) basins in the US.

2.5 Limitations for Operation

Power For standard installations, the BluBird unit requires solar power for continuous operation. The backup battery can operate the system for around 7 days with no solar power, or longer if the BluBird is remotely commanded to use a lower power setting for the air pump. As noted in Section 2.2.2.4, the unit will go into a sleep mode if voltage drops below 10V, allowing the battery to recharge, and then will automatically waken when sufficient power is available. Options exist to deploy a larger capacity battery or battery pack could be included, or the system can operate off AC power if available at the site.

Weather conditions The system can tolerate a wide range of weather conditions, as demonstrated by continuous operation in locations from west Texas to Massachusetts. Extremely high winds are a limitation, although at METEC's facility in Colorado during 2024 testing, most BluBird units on site withstood sustained winds of nearly 50 mph with peak gusts of 92 mph with no damage. Air temperatures are not a limitation except at extremes, although we have not experienced any failures that we can attribute to either low or high temperatures.. Based on testing, temperatures below -20 deg. F. can affect air pump operation. In such cases, the pump can be switched off temporarily. Other weather factors that come into play include

heavy snow, which will temporarily affect the solar panel and wind instruments. Build-up of ice rime on the wind vane and anemometer can also affect wind measurements. It is possible for some moisture to enter through the air intake in cases of very heavy rain during high winds.

Terrain BluBird monitoring is not affected by terrain, elevation, or vegetation, except to the extent that conditions modify the dispersion of gas, which may require adjusting dispersion assumptions in the emission rate calculations.

Distance from emission source As described in Section 4, gas concentration from an emission source decreases with distance from the source. The positioning of BluBird units needs to take into account the expected range of emission rates along with typical wind speeds. For leak rates typical of oil and gas operations (including small rates below 0.1 kg/hr), BluBird nodes should be deployed within about 100m of potential sources. However, when leak rates are relatively high (or methane is leaking from multiple locations), BluBirds can be effective even if positioned well away from the source(s). For example, BluBirds have detected leaks when the known source was at least 500m distant.

Communications To take full advantage of Earthview's system, BluBird nodes need to send data in real time to Earthview's cloud computing center. This requires either cellular coverage or connecting to an operator's local wireless network. Intermittent cell coverage is manageable using our approach of storing data on the node and then transmitting those data to the cloud when cell coverage is re-established, as described in Section 2.2.4.

Site access Installation and operation of the BluBird CMS requires no special types of access to field sites. Equipment is delivered by pickup truck, and is easily hand carried to desired placement locations. No drilling, driving of stakes, laying of cable, etc. are needed.

Nature of the site In normal operations (i.e.,the procedures outlined in Sections 3 and 4 below), to achieve expected methane measurement accuracies, each BluBird requires occasional exposure to air with a typical background concentration of methane (roughly 1.9 ppm). Situations that would be likely to violate this include placement indoors where there is a constant increased presence of methane and heavier VOCs, paint fumes, gasoline and potentially other pollutants, or outdoors use where these other pollutants are nearly constantly present. (There are options to use BluBirds in these settings, but non-standard data analysis procedures would be required.)

3 MOS Sample to Methane Concentration

Converting a BluBird sensor reading to a methane concentration in ppm involves sophisticated analysis, which is necessary to address the issues noted earlier (e.g., Sohn et al., 2007; Riddick

et al., 2020; 2022; Abdullah et al., 2022; Robianni et al., 2023), such as effects of humidity, temperature, sensor differences, and sensor drift. As noted earlier, this processing is how Earthview exploits the inherent high sensitivity of MOS sensors while minimizing the factors that can mask this sensitivity.

At a high level, this conversion can be described in the following steps, shown visually in Figure 22. Note Figure 22 was redacted as confidential business information.

1. Validate sensor data
2. Predict a clean-air MOS resistance
3. Calculate methane concentration from the ratio of observed to predicted MOS resistance using a response function that captures the relationship between resistances and methane concentrations.

[Confidential Business Information Redacted]

3.1 Validation

As discussed in Sections 2.1.2 and 3.2.1, the electrical resistance of MOS sensors is influenced by a variety of factors, but most predominantly humidity and temperature. If other sensors on a BluBird are reporting erroneous values, or if the voltage supplied to the MOS sensors is outside of acceptable range, the system cannot confidently convert the reading to a methane concentration. To circumvent this, all reads from a device are validated before they are converted to a methane concentration.

If a read fails validation, it is stored in the database for record keeping, but will not be converted to a methane concentration (invalid wind values can be replaced by other sources and do not invalidate methane concentration analysis). If a device in the field is continuously failing validation, it will be flagged for repair by the field operations team in the 6 hour automatic status reports. Table 8 lists automatic validation checks performed by the system, please note that Table 8 has been redacted as confidential business information.

[Confidential Business Information Redacted]

3.2 Predict Clean-Air MOS Resistance

3.2.1 Theory

MOS sensors detect gases by measuring changes in electrical resistance. When a target gas such as methane interacts with the MOS sensor, an induced change in the electrical resistance can be observed. The resistance across a MOS sensor can be affected by not only methane, but also by humidity, temperature, and other gases. These factors can cause variations in the sensor's resistance, making it challenging to isolate the effects of methane alone.

Below, we illustrate how this process allows detection of small changes in methane concentration. Figure 23 shows a time series of raw measured resistances (blue) and estimated clean-air resistances (orange) spanning about 16 hours. The raw resistances ("Rs") and the clean-air resistances ("Ro") correspond in the Rs/Ro vs. concentration relationship (i.e., the response function) to convert resistances to methane concentrations (Figure 25; See Section 3.3.1). This Rs/Ro ratio approach was also used by Eugster and Kling (2012); Maslanik (2014); Bastviken et al. (2020); Riddick et al. (2020), Maslanik et al. (2021), Shah et al. (2023), and others. In the example shown here, Rs varies from about 30000 ohms to over 70000 ohms over the period, due primarily to changes in humidity. If not accounted for, these swings would result in incorrect methane concentrations because increases in humidity result in a decrease in resistance, which mimics a decrease in resistance due to increased methane concentration. (In this example, if the atmospheric effects are not accounted for, the error is as great as 100 ppm). In Figure 23 and Figure 24, the small, high-frequency spikes in the measured resistances (plotted in blue) are typical of the effects of small amounts of methane, while the more gradual swings show changes in humidity.

This example demonstrates a critical point about our use of MOS sensors - it shows that the sensors are quite sensitive, as indicated by the fine-scale variations (the small spikes) seen in the time series. But this fine-scale signal is superimposed on a larger background pattern that varies more slowly. This general situation - where the presence of methane yields a typical spike pattern while humidity varies at a lower rate - provides one basis for separating the two influences on MOS resistances. This is a typical signal processing problem that can be tackled in multiple ways. The first step in Earthview's approach involves removing as much of this background as possible. This allows us to separate out the high frequency signal of methane spikes from the lower frequency changes in atmospheric background conditions.

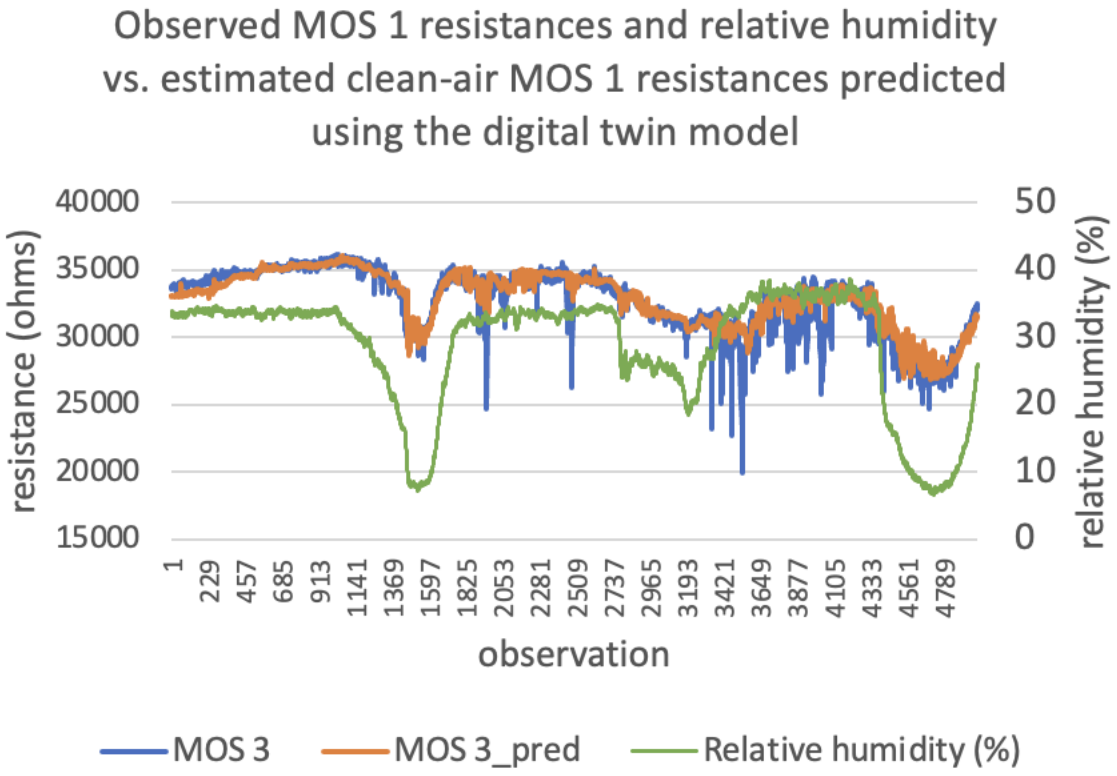

Figure 23. *Gas sensor measurements for a 32-hour period, with the measured MOS 1 resistances in blue, relative humidity in green, and the results of Earthview's proprietary adjustments for atmospheric conditions calculated using the MOS 1 sensor's digital twin model in orange (this is the Ro parameter referred to elsewhere in this document). Note how the Earthview-adjusted sensor readings account for the large-scale humidity effects, allowing extraction of the intermittent spikes associated with the presence of CH4.*

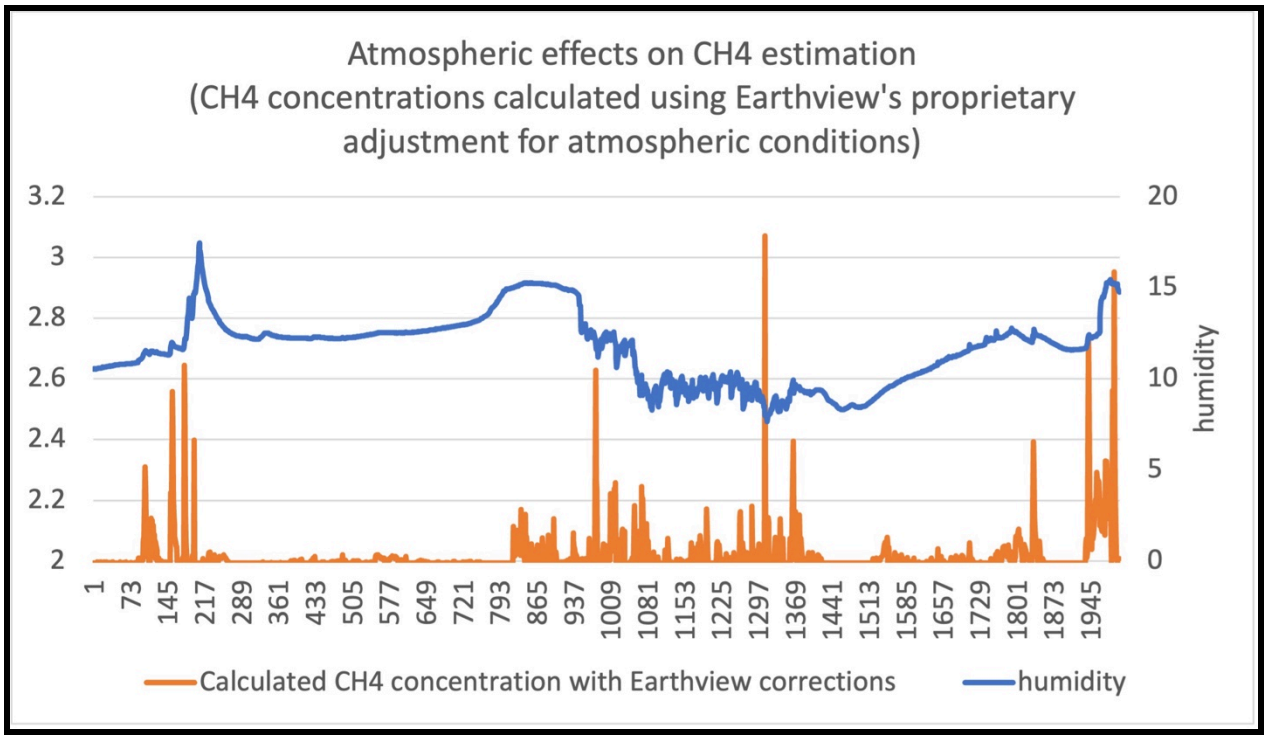

Figure 24. *Humidity plotted along with methane concentrations derived from sensor data adjusted using Earthview's methods to account for atmospheric effects. The large humidity effects are removed, allowing detection of small changes in CH4 concentration.*

3.2.2 Machine-Learning Based Digital Twin Sensor Model

It is generally assumed that MOS sensors require regular calibration to maintain accuracy in detecting gases (see theory discussion in Section 2.1.2.4.1). This would be the case when using MOS sensor resistances directly; for example, by fitting an equation to predict CH4 concentration as a function of MOS resistance, humidity and temperature (e.g., Furuta et al. (2022). However, as noted in sections 2.1.2.2 and 2.1.2.4, Earthview's approach takes a different approach, using the concept of a digital twin (Glaessgen and Starget, 2012; IBM, 2024) - a virtual model of a physical object. Earthview builds such a twin individually for each individual MOS sensor using real-time data (see Section 2.1.2.4.1).

The digital twin model accounts for the influence of environmental factors, and the effects of variations in humidity in particular. Digital twins are constructed for each individual MOS sensor in the field, using real-time data. They predict the expected clean-air resistance of the MOS sensor based on measured environmental conditions, humidity, temperature, etc. This

establishes a baseline resistance that the sensor should exhibit in the given conditions, without the influence of methane.

During operation, the resistances of the MOS sensors are measured in real-time. This observed resistance is compared to resistance predicted by the digital twin. The difference between the observed and predicted resistances indicates the portion of the resistance change that is due to the presence of methane. This difference is used later to calculate the methane concentration.

3.2.3 Machine Learning

Please note that the technique and details used to train and utilize machine learning is confidential business information and has been redacted.

[Confidential Business Information Redacted]

3.3 Calculate Methane Concentration

3.3.1 Response Functions

Once a predicted resistance is chosen, the ratio of observed resistance to predicted (clean-air) resistance is used to calculate the concentration of gas in the sample (e.g., Bastviken et al., 2020; Shah et al., 2023). The response functions for this calculation are displayed in the table below. As discussed earlier, this ratio refers to the observed/predicted resistance (Rs/Ro). These equations were developed by Earthview by fitting models to the Rs/Ro values plotted versus measured concentrations (e.g., Figure 25, Figure 26, Figure 27). A variety of data sets noted below have been used to develop these functions, including results in published literature, lab experiments with calibration gases, co-located field measurements with research-grade air monitoring instruments. Overall, we find that the response functions are quite consistent between different BluBird units.

Note that response functions and their development are confidential business information and have been redacted.

[Confidential Business Information Redacted]

3.3.2 MOS 1 and MOS 3 Sensors

To reiterate, the MOS 1 sensor is used for methane at lower concentrations, while the MOS 3 sensor is used for methane at higher concentrations. The separation point between using the MOS 1 or MOS 3 is confidential business information and has been redacted.

[Confidential Business Information Redacted]

3.3.3 Methane Concentration Accuracy

Below, we provide some examples documenting the sensitivity and accuracy of methane concentration estimates using data obtained in single-blind tests under field conditions. This includes testing done at a realistic oil and gas pad setting (Colorado State University's METEC facility) during ADED testing (e.g., Ilonze et al. 2024) and at an outdoors EPA facility. The estimated concentrations shown here encompass all of the Earthview processing steps described above. These steps include: (1) raw sensor measurements (Rs), (2) transmission to the Earthview cloud server, (3) real-time continuous auto calibration, (4) estimation of clean-air resistances (Ro), (5) calculation of resistance ratio Rs/Ro, and (5) conversion from Rs/Ro to methane concentration using standard Earthview algorithms. The results shown here are in line with results from other studies using the TGS2600 or TGS2611 MOS sensors (e.g., Van den Bossche et al., 2016; Bastviken et al. 2020; Torres et al., 2022; Shah et al., 2023).

3.3.3.1 Results from Natural Gas Releases in Outdoors Conditions - Concentration Estimates

Earthview conducted testing in 2021 using an array of 6 BluBird v.1 instruments positioned outdoors, downwind of a natural gas source released at 1.1 kg/hr, with wind speeds ranging from 0.8 m/s to 2.0 m/s (Maslanik and Givhan, 2021; see WP-2021-6 in Supplemental Materials). In this experiment, the BluBird system proved to be able to detect the 1.1 kg/hr emission of natural gas under light winds and at distances of 38m (the longest distance tested) and closer. The derived concentrations were reasonable as compared to expected concentrations for these conditions, and the measurements are relatively consistent between the 6 units. When the results are used to estimate a likely emission rate that would yield the BluBird-measured concentrations, the derived rates fall within the range of model uncertainty.

[Confidential Business Information Redacted]

3.3.3.4 Bench Testing Using Calibration Gas Mixtures

The results below were obtained by Earthview using methane calibration gas at different concentrations, obtained by mixing air zero gas with 1000 ppm methane to provide a range of known concentrations from near zero to 900 ppm. The BluBird measurements showed high correlation with the actual concentrations and good overall accuracy. Average error was 9% over a concentration range from 0-20 ppm, and 16% over a range from 0-900 ppm. ([Reference reserved as Confidential Business Information]).

The following figures show how BluBird responds to different concentrations of methane, using calibration gas mixtures and the LGD TDLAS for reference, with the airflow exiting the BluBird's sensor chamber routed into the Axetris LGD TDLAS to provide reference CH4 measurements. The BluBird concentrations were calculated using the MOS 1 "methane only (mo)" response function (which assumes near 100% methane in the gas mix) and a standard MOS 3 response function, which makes no assumptions about gas composition.

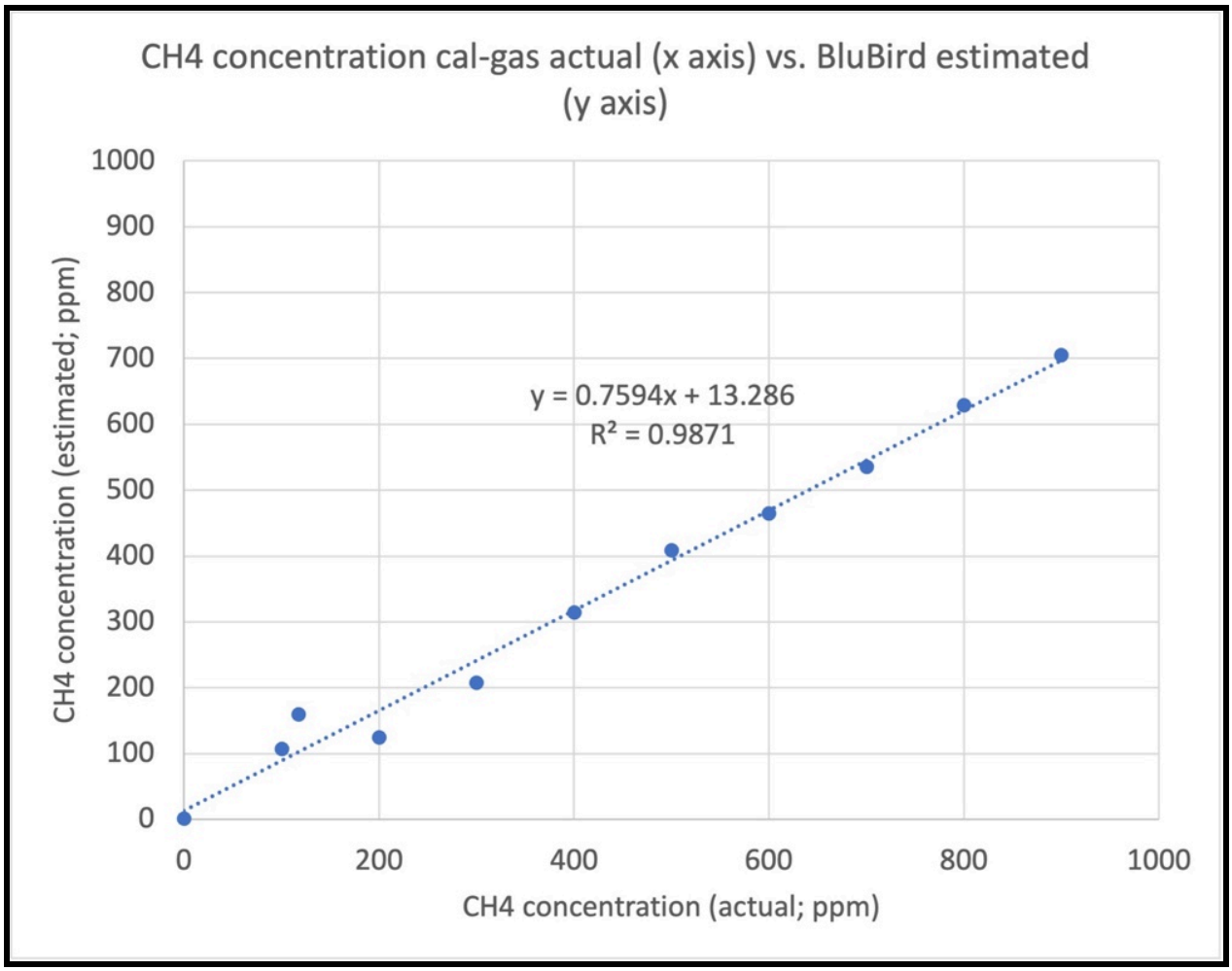
CH4 concentration cal-gas actual (x axis) vs. BluBird estimated (y axis)
CH4 concentration (estimated; ppm)
1000
900
800
700
600
500
400
300
200
100
0
y = 0.7594x + 13.286
R² = 0.9871
0
200
400
600
800
1000
CH4 concentration (actual; ppm)

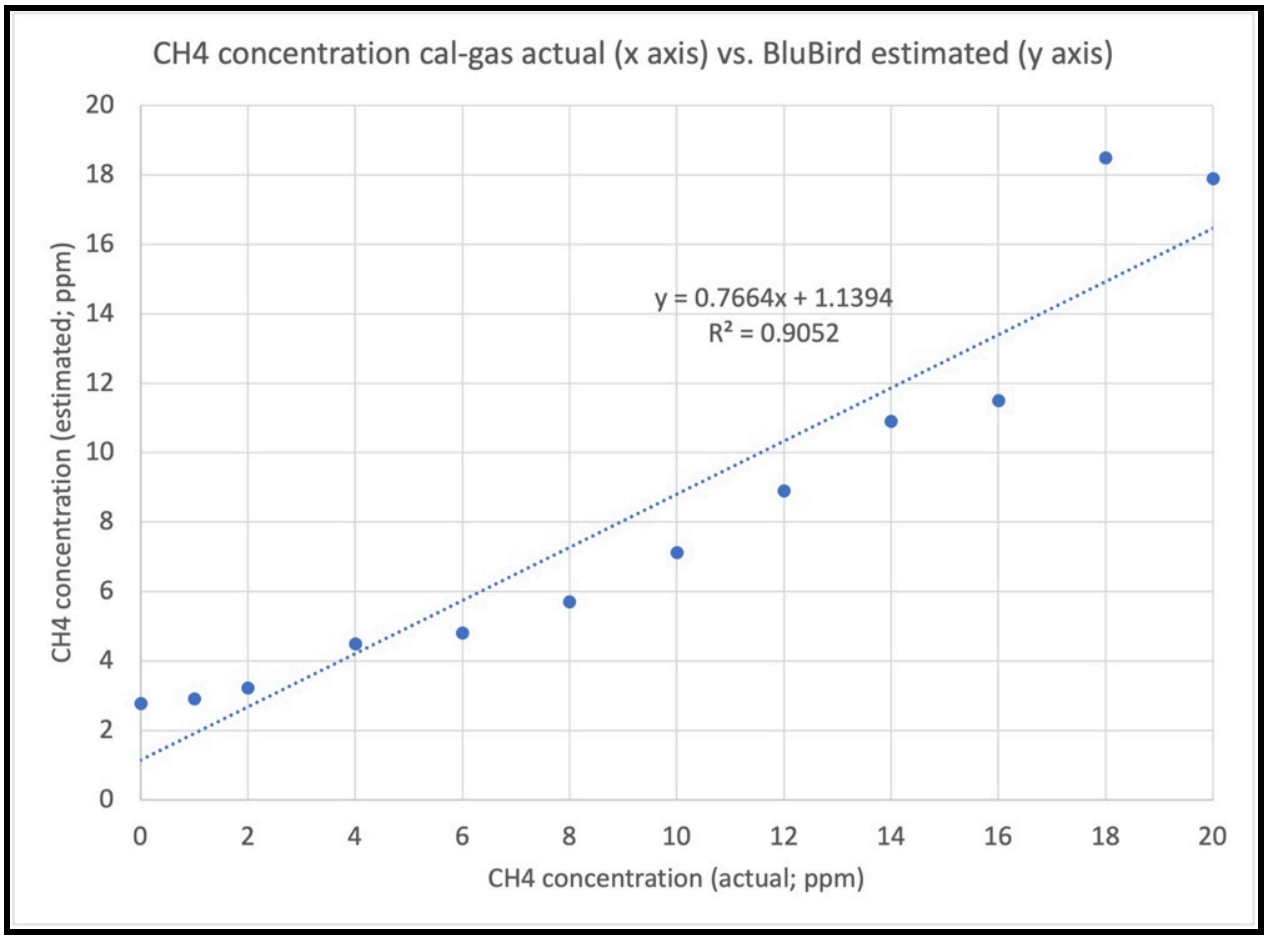

Figure 31. *Comparison of calibration gas CH4 concentrations with BluBird-estimated CH4 concentrations over a range from 0 to 700 ppm (top) and 0 to 20 ppm (bottom).*

We also have the ability to test how different combinations of natural gas constituents affect response function behavior (e.g., Figure 32). In this case, a 90% methane, 10% ethane mixture was generated using calibration gases. This mixture was then combined with zero air gas to produce a range of concentrations. This mixture was then supplied to a BluBird. The airflow exiting the BluBird's sensor chamber was routed into the LGD to provide reference CH4 measurements. Further analysis has been redacted as confidential business information.

[Confidential Business Information Redacted]

3.3.3.5 Co-located Measurements at an Air Quality Monitoring Site

Early in its development, the BlueBird sensor package (BluBird version 1) was deployed in the field in conjunction with research-grade instrumentation operated by Boulder A.I.R. LLC at two locations in Colorado (Broomfield Soaring Eagle Park and Boulder Reservoir; https://bouldair.com/). Methane is measured by Boulder A.I.R. using a Picarro G-2401 Cavity Ring Down Spectrometer. Results from these coincident observations are described in Maslanik (2021; see WP-2021-2 in Supplemental Materials). Figure 33 shows a comparison of Picarro and BluBird data for a 10 hour period. These results highlight the ability of the BluBird instrument to resolve small changes in concentration. (Since Boulder A.I.R.'s instruments are able to determine the concentrations of natural gas constituents (e.g., methane, ethane, propane, butane, etc.), we were also able to use these coincident measurements to quantify how the MOS sensor measurements varied with the presence of heavier non-methane VOCs.)

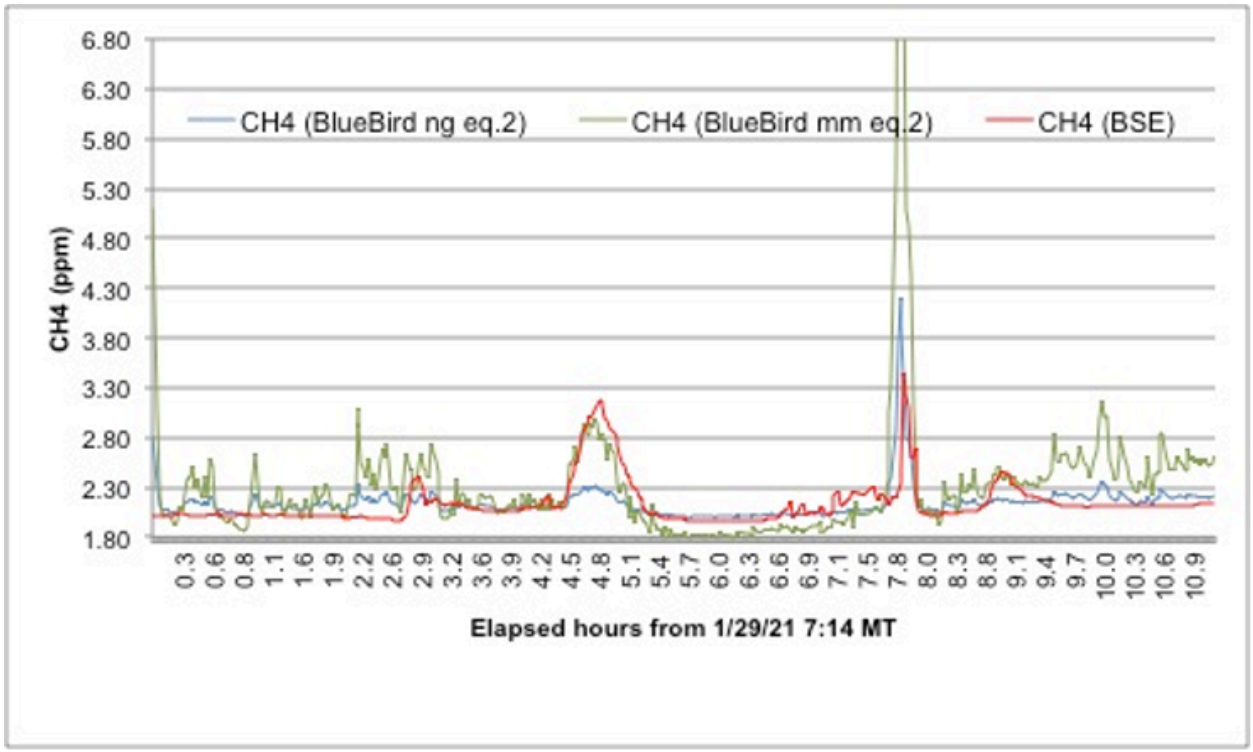

Figure 33: *Methane concentrations measured by the Picarro G-2401 (red) and methane concentrations estimated from BlueBird data using the "natural gas" equation (blue) and the "mostly methane" equation (green).*

4 Methane Concentration to Emissions Rate

There are several steps involved in converting a methane concentration to an emission rate. At a high level, a snapshot of a monitored location is taken every 10 minutes, where the measured methane concentrations are used to calculate emissions rates using plume dispersion modeling.

[Confidential Business Information Redacted]

4.1 Plume Dispersion Modeling

4.1.1 Inverse Gaussian Plume Model

As discussed in Section 2.1.3, Earthview uses the inverse version of the Gaussian plume model to estimate emission rate, along with modifications for special cases, as noted below.

The parts per million methane concentration can be converted to a grams per cubic meter concentration via the following equation, which takes the measured pressure and temperature into account:

c : methane concentration	$[g/m^3]$
c_{ppm} : methane concentration (parts per million)	$[1]$
P : atmospheric pressure	$[Pa]$
T : chamber temperature	$[K]$
R : ideal gas constant	$[J/K \cdot mol]$
M : molar mass of methane	$[g/mol]$

$$c = \frac{c_{\text{ppm}} P M}{10^6 R T}$$

Equation 5. Methane *parts per million concentration to grams per cubic meter concentration conversion.*

Here, we describe the exact formulations used for calculation.

$$
\begin{array}{ll}
q : \text{emission rate} & [g/s] \\
c : \text{methane concentration} & [g/m^3] \\
w : \text{wind speed} & [m/s] \\
h : \text{vertical distance between sensor and leak source} & [m] \\
x : \text{horizontal distance between sensor and leak source} & [m] \\
y : \text{horizontal distance from plume center} & [m] \\
z : \text{vertical distance from plume center} & [m] \\
A_y, B_y : y \text{ direction dispersion coefficients} & [1] \\
A_z, B_z : z \text{ direction dispersion coefficients} & [1]
\end{array}
$$

$$
q = \frac{2\pi c w \sigma_y \sigma_z}{f(y, \sigma_y)\left[f(z+h, \sigma_z) + f(z-h, \sigma_z)\right]}
$$

$$
\sigma_y = A_y x + B_y; \;\; \sigma_z = A_z x + B_z
$$

$$
f(r, \sigma) = \exp\left[-\frac{r^2}{2\sigma^2}\right]
$$

Equation 6. *Gaussian plume dispersion model.*

Plume dispersion modeling depends greatly on the choice of dispersion coefficients (e.g., Carrascal et al., 1993; Irwin et al., 2005; Finn et al., 2016), and many options for estimating the coefficients have been described in the literature (e.g., Korsakissok and Mallet, 2009). In our case, we use the dispersion coefficients provided in tables A-1 and A-2 in U.S. EPA (2013), as consistent with the OTM-33A approach. Using the data in the two tables, linear equations were fit to predict sigma y and sigma z as functions of distance between source and sensor. Individual equations were generated for each stability class. A and B in Equation 6 are the slope and intercept for each of the equations. Currently, our approach uses stability class parameters that are confidential business information and redacted.

[Confidential Business Information Redacted]

4.2 Localization and Quantification

As noted in Section 2.1, Earthview has developed the Gridded Pad Analysis and Quantification System (GPAQS) routines to carry out emission source localization and rate quantification. Details of GPAQS are provided below.

4.2.1. Spatial Resolution of the Technology

This ATM application is being submitted as a periodic screening technology that provides a facility-level spatial resolution. As described below, the BluBird system is able to determine the most likely locations of emissions sources, but this is typically limited to a resolution of 10m x 10m. The BluBird system is therefore being proposed as suitable for facility-level monitoring, which requires spatial resolution sufficient to identify emissions within the boundaries of the surveyed site. The material below documents this capability.

4.2.2 Grid Layout

The system that detects and quantifies ongoing leaks divides the area of potential leak locations into a grid of equally sized cells, typically 10m x 10m (Figure 35). If warranted by the site layout and number of nodes, the grid resolution can be increased to refine the estimated location. In the grid layout, green cells indicate a potential leak location and gray cells indicate locations without any known equipment.

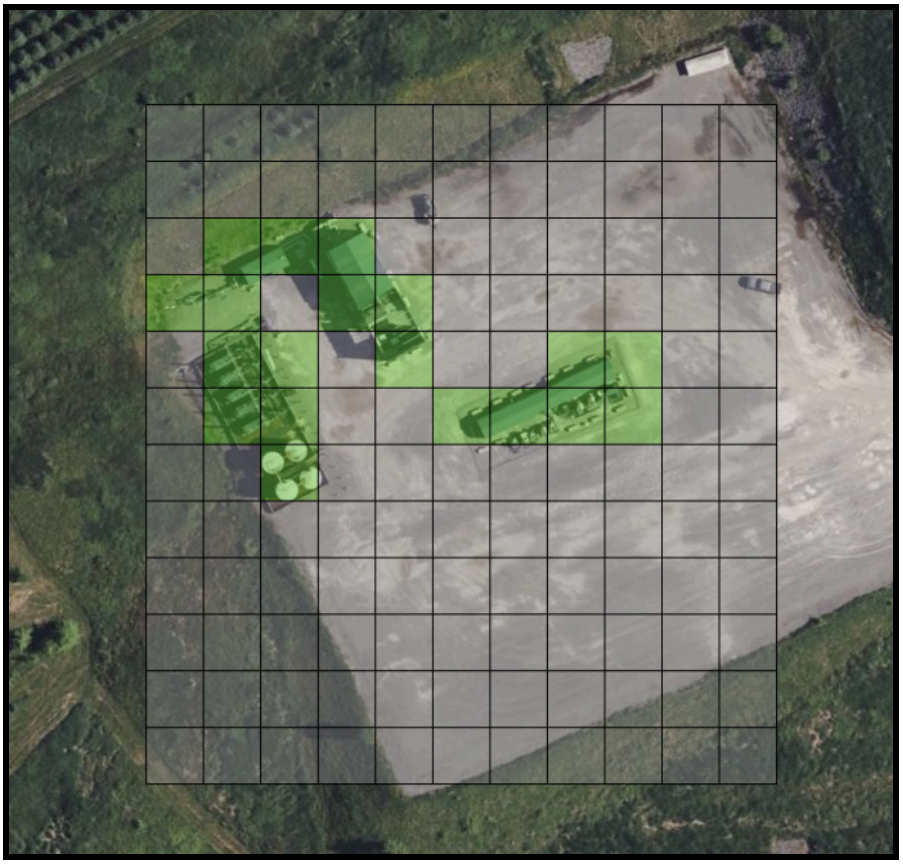

Figure 35*. Grid layout over potential leak locations. Green cells indicate a potential leak location (production equipment), gray cells indicate locations without any known equipment.*

4.2.3 Background Methane Concentrations

The detection system calculates a background methane concentration based on wind direction, device placement, and methane readings over a 10 minute sampling period. The details of background methane concentrations have been redacted as confidential business information.

[Confidential Business Information Redacted]

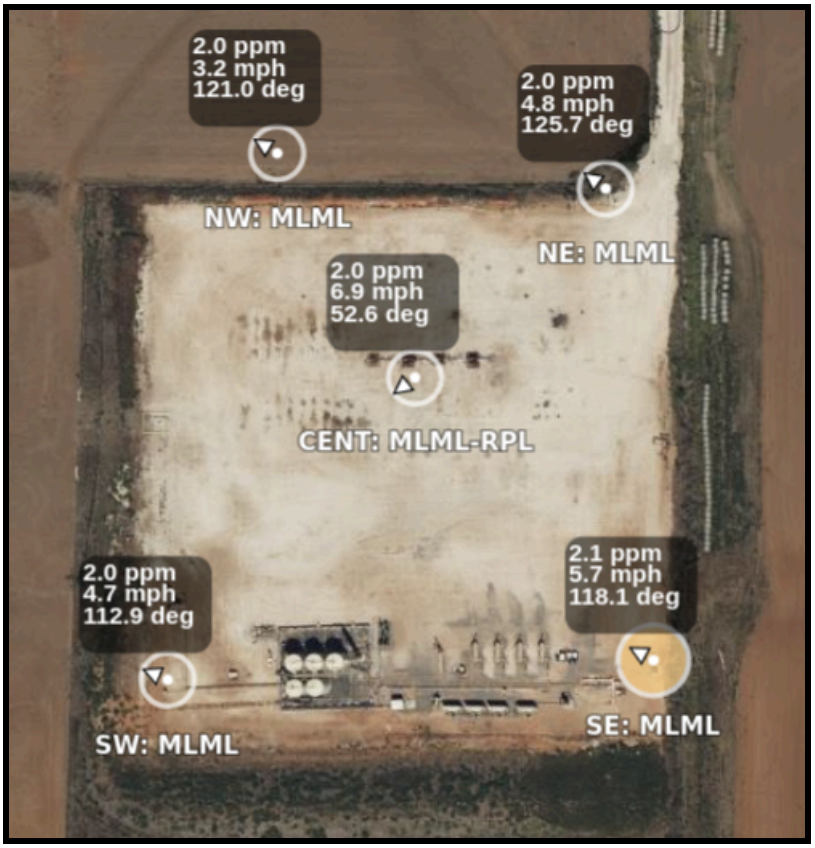

Figure 36*: Production facility with 5 sensors deployed.*

4.2.4 Leak Rate Quantification

The detection system calculates emissions rates every 10 minutes. The exact methodology of leak rate quantification has been redacted as confidential business information.

[Confidential Business Information Redacted]

4.2.5 Localization

Localizing leaks is confidential business information and has been redacted.

[Confidential Business Information Redacted]

4.3 Emission Action-Level Analysis for Periodic Screening

This application seeks approval of the Earthview GMS for use as a periodic screening technology. This requires demonstrated ability to detect emissions above the thresholds listed in CFR §60.5397b(c) tables 1 and 2. These tables list the minimum detection thresholds at 90% probability of detection (POD) that the alternative test method must offer, in terms of different screening frequencies.

Periodic screening per 40 CFR §60.5398b(b) requires that all portions of the site be observed during a survey. To achieve this, Earthview's system measures site emissions for enough time to allow every grid cell on the site to be "seen" by at least one BluBird node. Here, this is defined as the wind direction aligning such that a vector drawn from a grid cell intersects a node. Once all parts of the site portions of the site have been sampled in this manner the average emission rate for the site as measured over the survey period is calculated and checked to see if target emission thresholds have been exceeded. The survey results are provided to the operator within 24 hours of completion of the survey period.

The above screening procedure is designed to mimic as closely as possible an "emissions snapshot" of the site; comparable to that provided by an aircraft overpass. However, since the BluBird system calculates emissions continuously, there are variations of the above procedure that could be applied if EPA modifies or further defines the survey requirements for periodic screening using continuous monitoring data. For example, emission rates could be averaged over a longer time period, or rather than using an average, the maximum emission rate over the survey period could be determined. Another option would be to use identified emissions events or emissions above an emissions baseline for the site.

Since Earthview's 90% POD levels cited here are based on METEC ADED testing, applicability of these levels to field sites requires that the BluBird installations be consistent with those during ADED. The main requirement is that all potential sources of emissions be within 100m of a node. This is dictated by the range of methane concentrations expected to be encountered under typical weather conditions for an emission rate of at least 1 kg/h (or 3 kg/h during the first 3 years of the program). (Note: for other, higher, emission thresholds listed in paragraphs 40 CFR 60.5398b(b) and/or (c), the required minimum distances can be greater.)

One survey is to be done in this manner quarterly for well sites, centralized production facilities, and compressor stations subject to AVO inspections with quarterly OGI or EPA Method 21 monitoring, or semiannually for well sites and centralized production facilities subject semiannual OGI or Method 21 monitoring.

EPA's guidelines in Subpart OOOOb of Part 60, tables 1 and 2 are based on the monitoring technology's minimum detection threshold, as defined by the emission level that is demonstrably

detectable 90% of the time by the screening technology. This is typically referred to as the 90% Probability of Detection (POD) level. The proposed ATM's cited 90% POD levels are based primarily on Colorado State University METEC Advancing Development of Emissions Detection (ADED) testing. Therefore, the BluBird node installations should provide comparable sampling capability. To achieve this, potential sources of emissions should be within approximately 100m of a node. This is dictated by the range of methane concentrations expected to be encountered under typical weather conditions for an emission rate of at least 1 kg/hr.

If periodic screening survey detects confirmed emissions above the relevant thresholds listed in Part 60 tables 1 and 2, the operator is required to investigate the emissions as described in 40 CFR 60.5398b(b)(5). The ATM system supports this in various ways that can be useful to the operator. For example, daily emission estimates can be provided, which the operator can use to monitor progress of repairs and to document that requirements have been met.

4.3.1 Probability of Detection

Much of the following information is based on Earthview results achieved during single-blind testing at the The Colorado State University Methane Emission Technology and Evaluation Center (METEC) facility as part of the Advancing Development of Emissions Detection (ADED) program, which was carried out during February - April 2024 (METEC, 2024; Maslanik et al., 2024 [white paper WP-2022-3 in Supplemental Materials]),

CFR §60.5397b(c) tables 1 and 2 list the minimum detection thresholds at 90% probability of detection (POD) that the alternative test method must offer, in terms of different screening frequencies. The minimum detection threshold with 90% probability of detection (POD) that is specified is ≤ 5 kg/hr. As described below, the Earthview BluBird GMS has demonstrated the ability to detect 1 kg/h at a 90% POD. This POD claim is based on recently completed testing at the CSU METEC facility as part of the Advancing Development of Emissions Detection (ADED) program, which was carried out during February - April 2024. This claim is also supported by performance at actual field sites.

METEC's standard method of assessing leak detection performance during previous ADED experiments (e.g., Ilonzi et al., 2024) uses a methodology that arguably is not well suited to assessing continuous monitoring solutions. METEC has since developed a new testing and grading protocol that will be used for future ADED experiments from 2025 onward (METEC, 2025). The results presented below are from an analysis of Earthview BluBird ADED 2024 performance using grading criteria that are consistent with this ADED 2.0 protocol (E. Levin, pers. comm.). Specifically, a detection report that significantly overlaps a METEC release is classified as a successful detection, and any detection of one or more leaks during a multi-release experiment is considered as a successful site-level detection.

In terms of total event (i.e., experiment) detection, using these revised ADED 2.0 criteria, 98% (343 of 349) of METEC's site-level events were automatically detected and reported. Ninety-three percent (53 of 57) of site-level events of less than 0.4 kg/hr were detected, with a minimum detection level of 0.04 kg/hr. (For cases with more than one release per experiment, the maximum release rate was used for analysis). Leak event duration was accurately determined, with average durations of 229 minutes versus METEC's average of 224 minutes (Maslanik et al., 2024b; WP2022_3.pdf in Supplemental Materials).

A commonly applied method for defining POD uses binary classification methods such as logistic regression modeling to identify the relationship between whether a leak was detected, as a function of some parameter such as leak rate. Using these criteria, this approach yields a 90 %POD for releases of 60 g/hr or greater (Figure 39). The predictive power of the model is relatively weak,suggesting that the BluBird GMS' leak detection rate is not strongly dependent on emission rates. This can be explained by the fact that the BluBird system is quite sensitive, and is able to detect sub-ppm increases in CH4 concentrations. As described in the next section, leak rates greater than around 0.4 kg/hr are likely to yield CH4 increases that are detectable by BluBird under typical field deployments.

Given this ability to detect low concentrations, other factors such as leak duration or total emission during an event are likely to be more relevant for BluBird POD. In fact, the time required for wind direction to align between a leak source and a sensor node is the main control on whether a leak will be detected. This is controlled by variability in wind direction along with the placement and number of nodes. It is important to note that, for the ADED 2024 results presented here, Earthview had deployed 12 nodes. This is more than would be typical for an oil and gas production pad (a typical Earthview deployment ranges from 4 to 10 nodes, depending on site complexity and customer preferences) but is intended to compensate for the fact that METEC's release rates are relatively short, so less time was available for winds to intersect nodes, and that METEC released gas from up to 5 different locations at a time on the test pad.

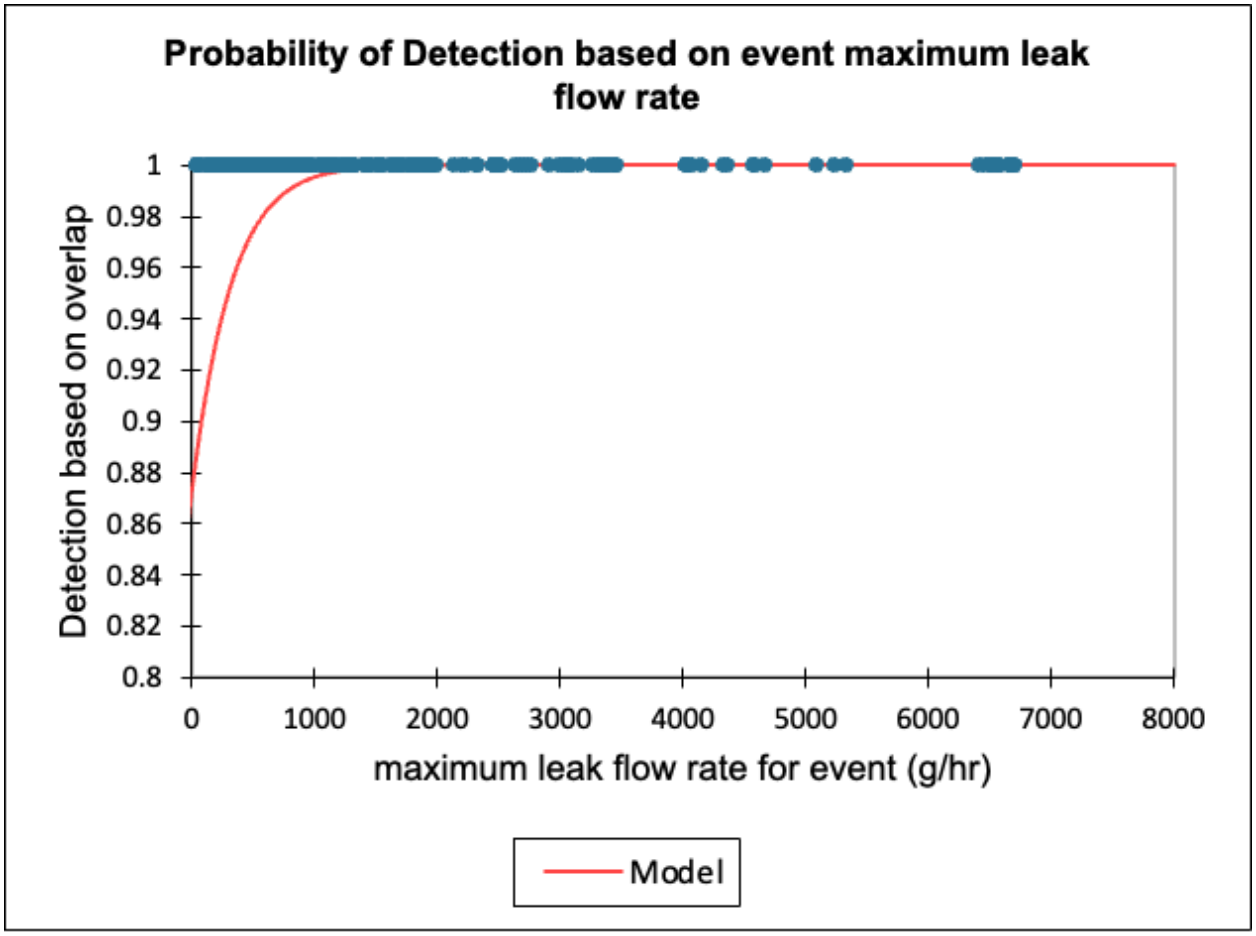

Figure 39. *Probability of detection estimation using logistic regression applied to event maximum leak-flow rate (quantitative parameter) with overlap-based detection flag as the response parameter. The POD reaches 90% at a leak flow rate of 90 g/hr.*

Using the same "overlapping detection" criterion, BluBird's POD was 97% (100 of 103) single-release events. For these single-release events, the statistical POD is above 90% for the full range of event release rates (Figure 40).

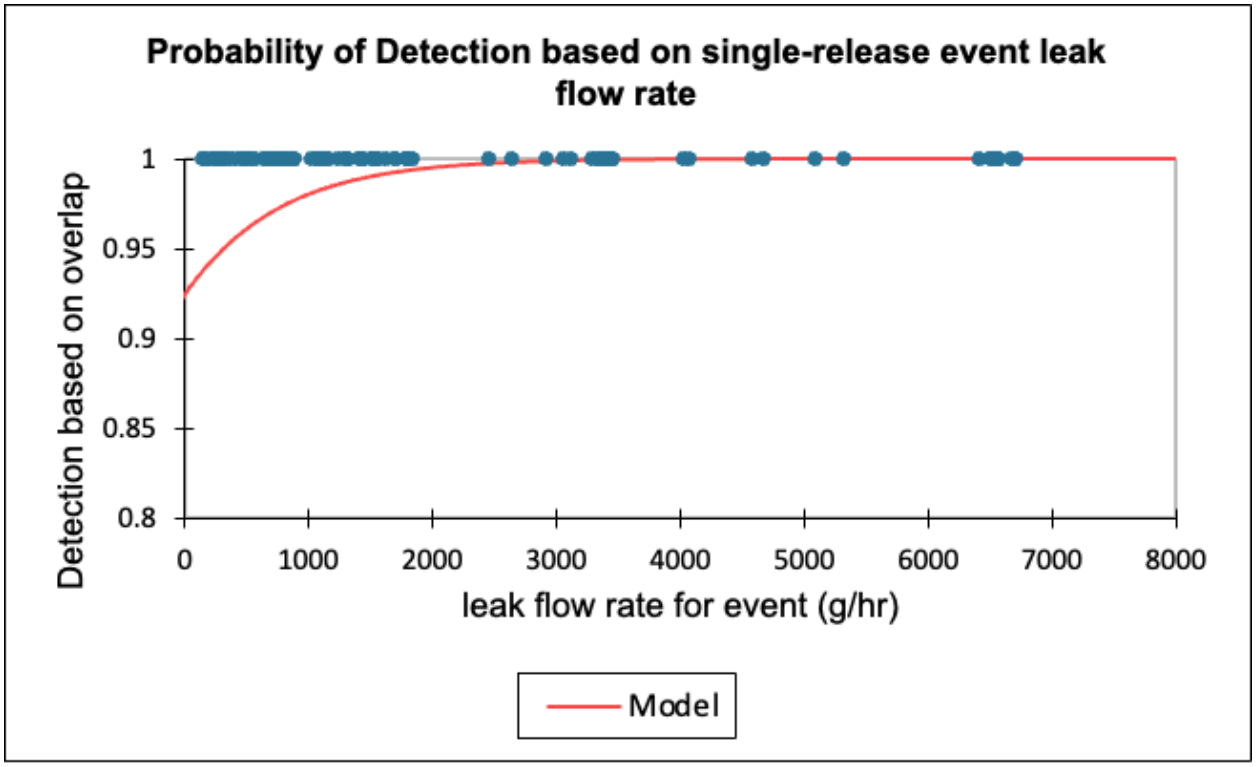

Figure 40. *Probability of detection estimation using logistic regression applied to single-release event leakflow rate (quantitative parameter) with overlap-based detection flag as the response parameter. The POD is above 90% for the full range of event release rates.*

While METEC ADED testing focuses on detection rate as a function of leak rates, for point sensors such as BluBird that have a high sensitivity, the detection rate is controlled mostly by the time it takes for wind direction to align with the leak source and a sensor node. Therefore, POD is affected both by release rate and by leak duration. One way to represent this is by calculating the total gas release during experiments (e.g., release rate multiplied by release duration). This relationship is depicted in Figure 41. This POD plot suggests that a leak yielding at least 3800 grams should be detectable at the 90% level under conditions comparable to the ADED testing. In other words, at a leak rate of 1 kg/h, the leak might be expected to be detected within a maximum of 4 hours.

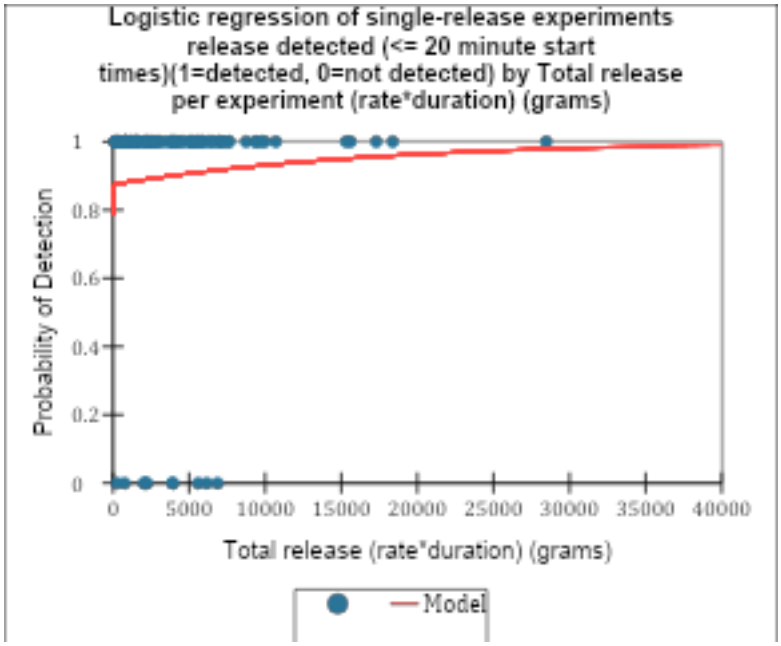

Figure 41. *Probability of detection as a function of total natural gas released during experiments. Detection reports meeting the 20-minute start time threshold were included.*

4.3.2. Baseline Emission Rates

Earthview's standard processing also includes automatic estimation of baseline emission rates for all sites. This is not required for periodic survey methods but provides an additional helpful tool to site operators for monitoring site behavior, including effectiveness of repairs and changes due to equipment modifications.

4.3.3 Data in Support of Action-Level Investigative Analysis

If a periodic screening survey detects confirmed emissions above the relevant thresholds listed in Part 60 tables 1 and 2, the operator is required to investigate the emissions as described in 40 CFR 60.5398b(b)(5). The BluBird system supports this in various ways that can be useful to the operator. For example, daily emission estimates can be provided, which the operator can use to monitor progress of repairs and to document that requirements have been met.

4.4 Measurement Uncertainty

To quantify the uncertainty in emission rate calculations, we need to consider the individual uncertainties inherent in the measurement equipment. These calculations involve multiple inputs and relatively complex nonlinear equations, which make the mathematical determination of propagated uncertainty difficult. The methods for calculating uncertainty are confidential business information and have been redacted.

[Confidential Business Information Redacted]

4.5 Verification

The biggest uncertainty in quantification is localization. For example, a leak that produces a certain concentration of methane measured from 3 meters away will be considerably smaller than a leak that produces the same concentration at, say, 100 meters away. The way that Earthview circumvents this is by getting verification from customers about the location of the source. The BluBird CMS system is designed to detect leaks and notify the customer of the most likely source, but without verification there is no closing of the loop to confirm where the leak originated from.

When operators respond to an alert they are given an email and report in the Earthview dashboard on the two most likely sources. An Example email is displayed in Figure 42 and an image of the likely leak sources is displayed in Figure 43.

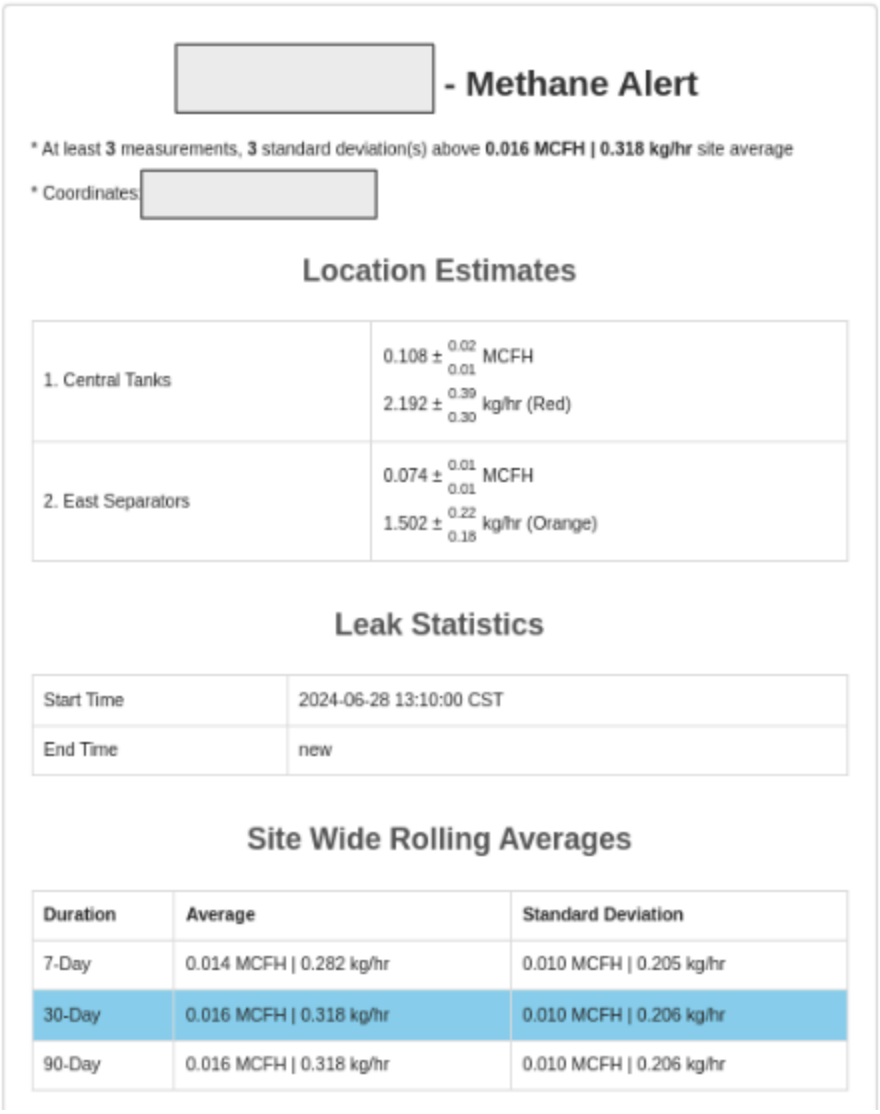

[redacted] - Methane Alert

* At least **3** measurements, **3** standard deviation(s) above **0.016 MCFH | 0.318 kg/hr** site average

* Coordinates: [redacted]

Location Estimates

1. Central Tanks	$0.108 \pm {}^{0.02}_{0.01}$ MCFH $2.192 \pm {}^{0.39}_{0.30}$ kg/hr (Red)
2. East Separators	$0.074 \pm {}^{0.01}_{0.01}$ MCFH $1.502 \pm {}^{0.22}_{0.18}$ kg/hr (Orange)

Leak Statistics

Start Time	2024-06-28 13:10:00 CST
End Time	new

Site Wide Rolling Averages

Duration	Average	Standard Deviation
7-Day	0.014 MCFH | 0.282 kg/hr	0.010 MCFH | 0.205 kg/hr
30-Day	0.016 MCFH | 0.318 kg/hr	0.010 MCFH | 0.206 kg/hr
90-Day	0.016 MCFH | 0.318 kg/hr	0.010 MCFH | 0.206 kg/hr

Figure 43. *Example email notification that goes out to customer when event detected*

Figure 44. *Example localization estimates sent in event notifications that are sent out to customers.*

The customer will respond to the event and verify that a leak was a true positive or false negative. In the true positive case the customer will triage in the dashboard where the leak originated from and Earthview can back calculate what the emissions rate was with the known source, thereby obtaining the most accurate emissions estimate possible. Furthermore, users can classify events into one of three categories, maintenance, operational and fugitive.

4.6 Emission Rate Quantification Accuracy

Studies using inverse Gaussian plume modeling to calculate point emission rates from oil and gas facilities typically suggest accuracies of about +/- 0.3 to +/- 2.0, [(estimated emission rate-actual release rate]/[actual release rate]). Edie et al. (2020) reports an accuracy of +/- 0.7 for 95% of observations using the OTM 33A mobile approach carried out at the METEC facility, using releases from single and multiple sources. Sixty-eight percent of the rates are within 38% of the known release rates. Combining their test results with those of similar testing done by Robertson et al. (2017), Edie et al. found that greater than 85 % of the calculated emission rates are within ±50 % of the known rate, and 95 % of the estimated rates are within ±73 %. The Earthview's performance cited below are consistent with these OTM 33A results.

4.6.1 Results from Natural Gas Releases in Outdoors Conditions - Emission Rate Estimation

Earthview's standard processing methods, including automatic baseline calibration, were applied to the natural gas release experiment described in Maslanik and Givhan (2021) to estimate emission rates using a range of atmospheric stability classes and source-to-sensor distances, for a known emission rate of 1.1 kg/hr. Estimated rates were 0.4 kg/hr if neutral stability conditions were assumed, to around 2 kg/hr if mixing conditions were moderately unstable (the most likely condition at the time) to 6.1 kg/hr for extremely unstable conditions. Overall conclusions are that the BluBird v. 1 system was clearly able to detect the 1.1 kg/hr release at a distance of at least about 40 m, with quantification accuracy consistent with our expectations based on other work (e.g., Riddick et al., 2020).

4.6.2 Single-Blind METEC ADED 2024 Results - Emission Rate Estimation

The best data we have for estimating emission rate accuracy with the BluBird system for actual field conditions are the results from the METEC ADED 2024 Feb. - April test period (METEC, 2024). The results have been redacted as confidential business information.

[Confidential Business Information Redacted]

4.7 Performance Metrics

The ATM application guidelines list several specific criteria that the proposed alternative monitoring method is expected to provide. Among these are the ability to measure relatively small increases in emission rates, and demonstrated probability of detection levels. Below, we focus on these and related performance measures. Much of the following information is based on confidential business information that has been redacted.

[Confidential Business Information Redacted]

4.7.3 List of Actual Leak Detections as Confirmed by Customers

Earthview has successfully detected numerous emissions events at our customers' sites. A list is displayed in Table 18.

Earthview has successfully detected numerous emissions events at our customers' sites, with the large majority of these having been confirmed by the customers during subsequent LDAR inspections. Several of these events were at rates of 1 kg/hr or less. A partial list of these events is available in the detected_confirmed_emissions_events.pdf table in Supplemental Materials. Below is an excerpt from this table, which presently lists over 60 such events.

Examples of BluBird-detected emission events confirmed by customers within the past 18 months (October 2022 - August 2024). (Entries in quotes are direct statements received from customers. Emissions alerts are typically set at a minimum rate of 0.1 MCFH [~1.8 kg/hr]) or less. (These are only a subset of the detected events.)

Date and Location	Earthview-Estimated Emission Rate	Operator's Confirmation
8/15/2024; Texas	high concentration alert**	"midstream company purging their line"
8/14/2024; Pennsylvania	1.3 MCFH	maintenance release from separators
7/10/2024; Texas	high concentration alert	"Hung dump valve so dumping gas to tanks"
6/19/2024; Texas	high concentration alert	"Hung dump valve, so was full Gas stream to tank. Discovered with Earthview alert first. Scada caught it but just the way it polls we noticed with Earthview first."
6/18/2024; Texas	0.2 MCFH	"Found a leaking dump control in SW corner."
6/11/2024; Texas	0.03 MCFH	"One of the pneumatic pumps at wellhead pumping chemical had a small constant leak "
5/19/2024; Texas	1.3 MCFH	"hung dump valve on compressor"
5/11/2024; Texas	high concentration alert	"Was a hung dump valve. Had pumper go by early and found it."
5/11/2024; Texas	0.1 MCFH	leaking regulator
4/11/2024; Pennsylvania	1.6 MCFH	"venting on a well"
4/9/2024; Oklahoma	0.7 MCFH	Earthview confirmation***

Table 18. Excerpt from Earthview-maintained list of detected and confirmed emission events (see detected_confirmed_emissions_events.pdf table in Supplemental Materials).

5 Security and Data Flow

5.1 Data Flow

5.1.1 Collection

BluBird Data

- Sample data
  - MOS resistances
  - Wind measurements
  - Environmental information such as temperature and humidity
- GPS data
  - Latitude & longitude, sent every hour
- Device health information
  - Battery Voltage
  - Cell signal quality
  - If device was opened

Weather Data

- sourced from https://www.weatherapi.com/
  - Ambient temperature, humidity, pressure
  - Wind speed and direction (used for comparison of local instruments/backup data)
  - Cloud Coverage

5.1.2 Analysis

Methane Concentration

- Conversion from MOS readings to methane concentration

Emissions Estimates

- Conversion from methane concentration, environmental data and localization analysis to methane leak rate

Events

- Aggregation of emissions rate estimates over time to determine emission duration

5.1.3 Storage

Earthview stores data using a variety of methods. Relational data that deals with users, devices and site assignment is done with a Relational PostgreSQL database. Timestream data such as sensor reads and methane concentrations are stored in AWS Timestream and DynamoDB NoSQL databases. Documents and temporary files are stored in AWS S3. Earthview does not store any Personal Identifiable Information (PII).

5.1.4 Availability

Data is made available to end-users via an API and through downloading CSVs through the Earthview Dashboard.

Earthview's API is documented in a swagger file located at https://docs.earthview.io/swagger.

- **Daily Emissions** - Daily summation of all events for a given site.
- **Alarms** - Individual events generated at a given site on a specific day.
- **Sites** - Locations Earthview is currently monitoring per client organization.
- **Node PPM** - Minute-by-minute methane concentrations recorded at a given site.

5.2 Security Policies and Documentation

Earthview utilizes a cloud based software architecture that leverages zero trust security to grant devices and users the least amount of privilege necessary to perform their roles. In a cloud based architecture our vendor, Amazon Web Services (AWS), takes responsibility for the cloud. This involves all on-premise level security, such as hardware, servers, networking etc. Earthview is responsible for security in the cloud. This includes securing client data, networking, firewall configurations, encryption etc. AWS's shared security model is outlined in Figure 52.

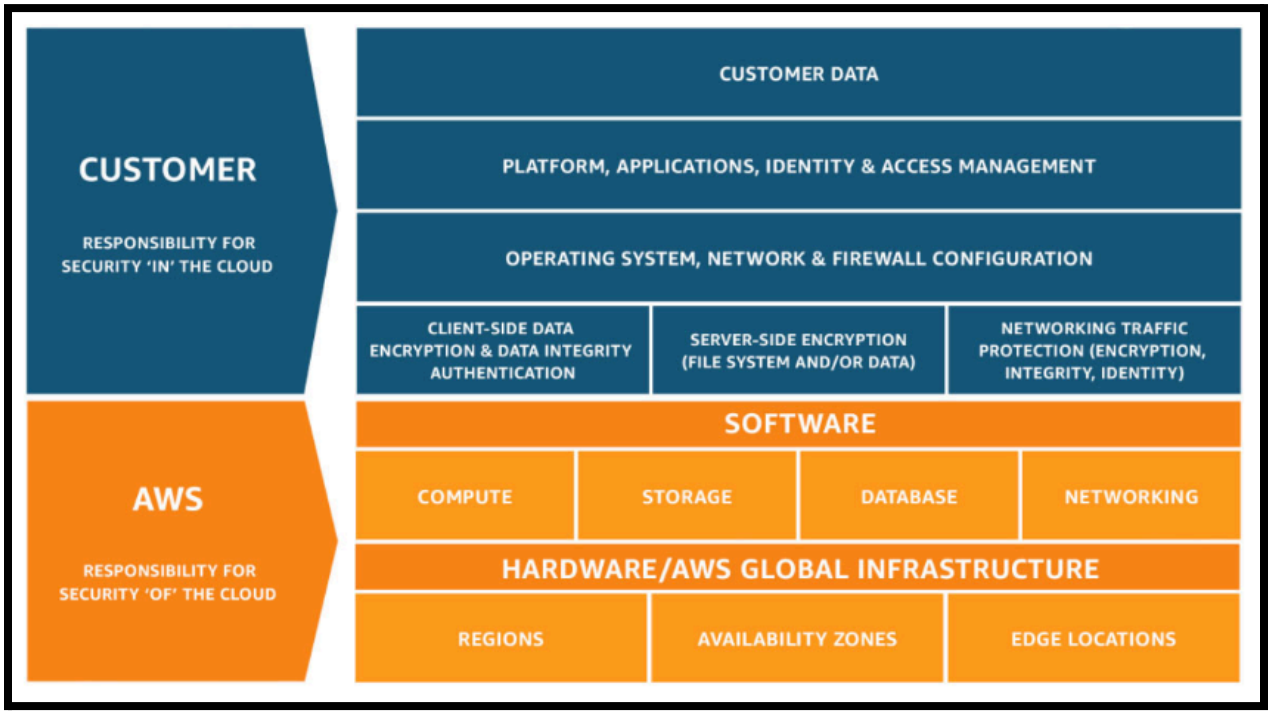

Figure 52. *AWS shared security model outlining the responsibilities of AWS vs the Customer. (“Shared Responsibility Model - Amazon Web Services (AWS)”)*

5.2.1 System Security

- **Authentication and Access Control:** All devices authenticate using an advanced algorithm that is unique and secure for each session. Access to the system is granted based on the privilege of least privilege, ensuring users and devices only access the portions of the system necessary for their role.
- **Network Security**: AWS VPCs are used to isolate data from the internet. Security groups and network Access Control Lists (ACLs) configured to restrict traffic to only trusted IP addresses and ports.
- **Data Encryption:** All data in transit and at rest is encrypted using strong encryption standards. HTTPS/TLS for data in transit and AES-256 for data at rest. AWS services such as S3, RDS and DynamoDB are configured to use encryption at rest.

5.2.2 Device Security

- **Device Provisioning:** IoT devices are provisioned securely to communicate via HTTPS/TLS to securely communicate with devices and prevent unauthorized access.
- **Firmware Updates:** IoT devices support over-the-air (OTA) updates to ensure that firmware can be updated promptly to patch vulnerabilities.
- **Physical Security**: Devices are equipped with switches that alert Earthview if they are ever opened, and GPS instruments to inform the team of a device's last position in time.

5.2.3 Access Management

- **IAM Policies**: AWS Identity and Access Management (IAM) roles and policies are implemented to control access to AWS resources. Roles are assigned based on job responsibilities, and IAM policies are reviewed periodically to ensure they align with the principle of least privilege.
- **Logging and Monitoring:** AWS CloudTrail and Cloudwatch are used to log and monitor all API calls and system activity in a centralized auditable location. Alerts are configured for failures and suspicious activity.
- **User Access:** Cognito User Pools used to grant Bearer Access Tokens to users to access APIs and the Earthview Dashboard. Users are only given access to their particular organization's data. Application security in place to deny unauthorized access to any clients data besides their own.

5.2.4 Incident Response

- **Backups**: Snapshots of data stored in Relational Databases, NoSQL, S3 are taken daily. In the event of an incident these snapshots can restore data and application performance with minimum downtime.
- **Resources:** Earthview defines resources used in cloud environments as code also known asInfrastructure as Code (IaC). In the event of a regional outage, resources could be stood up in another area of the country with minimal downtime.

5.2.5 Security Architecture

- High Level architecture can be viewed in Figure 53 below.
- All communication is done in SSL.
- Data is encrypted and isolated in a private VPC that does not have access to the internet.
- Access between the users and devices, and application is all done through APIs.
- Users are authenticated using Cognito User Pools and granted temporary credentials.
- Devices are authenticated with a unique secure algorithm.

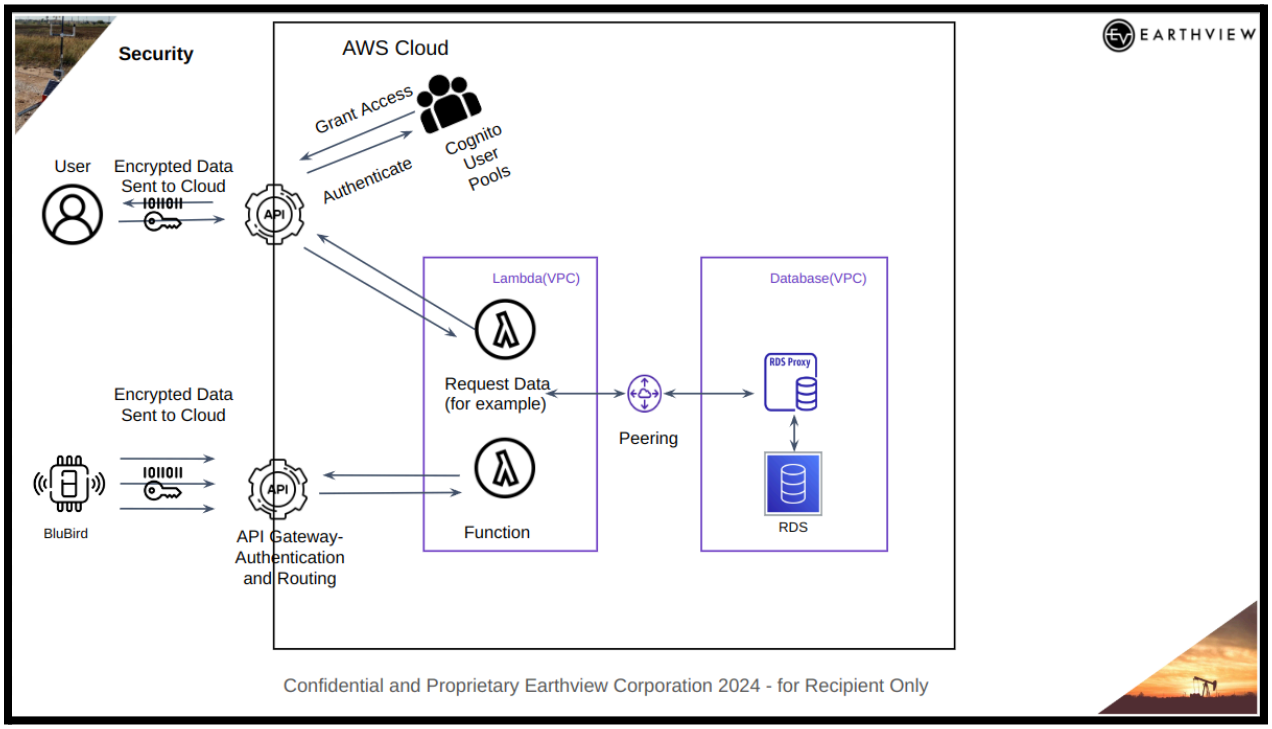

Figure 53. *High level security cloud architecture.*

- **Dashboard and API Authentication**

- **Bearer Authentication**
  - Access tokens granted to users and devices after verification of login credentials
  - Tokens expire in 1 hour and are continuously monitored for usage

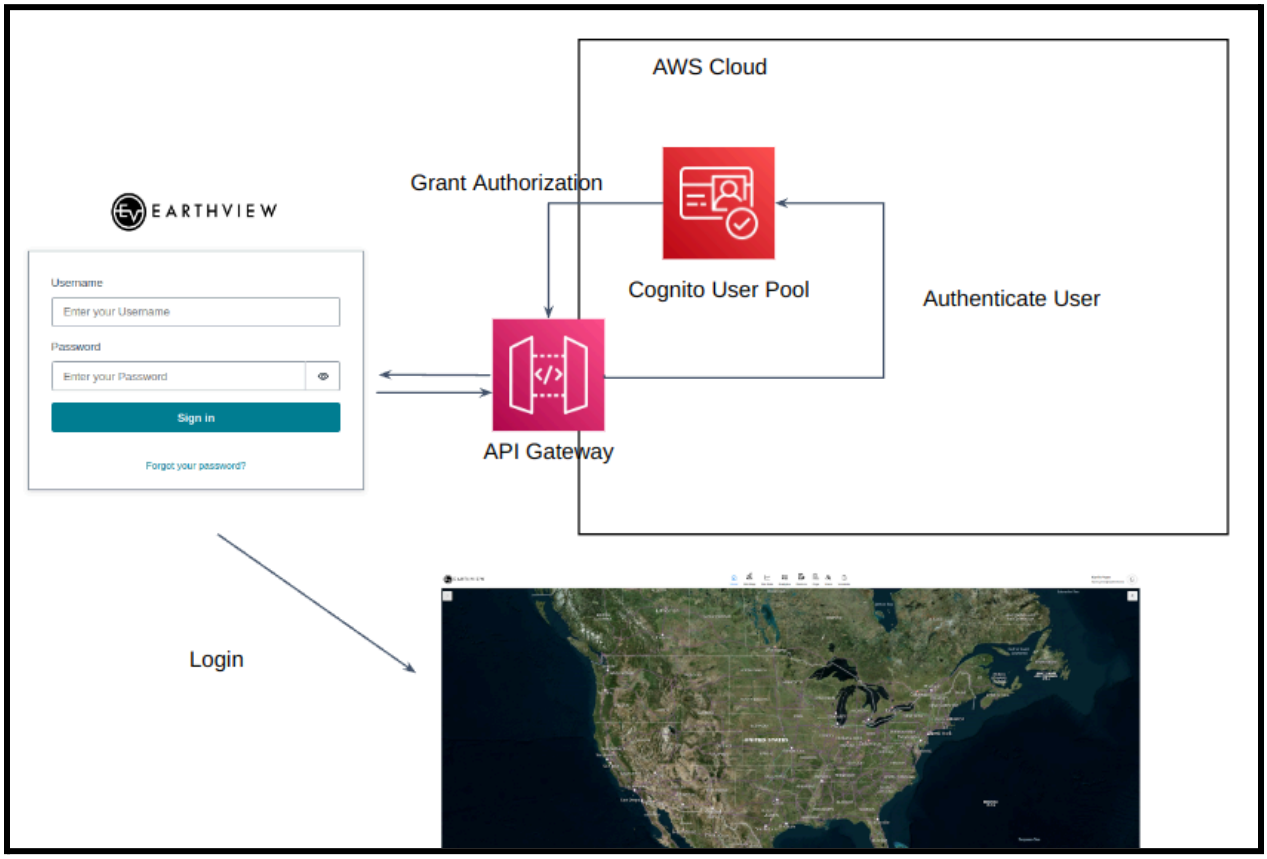

Figure 54*. Bearer Authentication login flow for a user logging into the Earthview Dashboard or using the API.*

- **Single Sign On (SSO)**
  - For a more secure and streamlined user experience Earthview has implemented Single Sign On (SSO)
  - This requires integration to clients Identity Provider (IdP)
  - See Figure 55

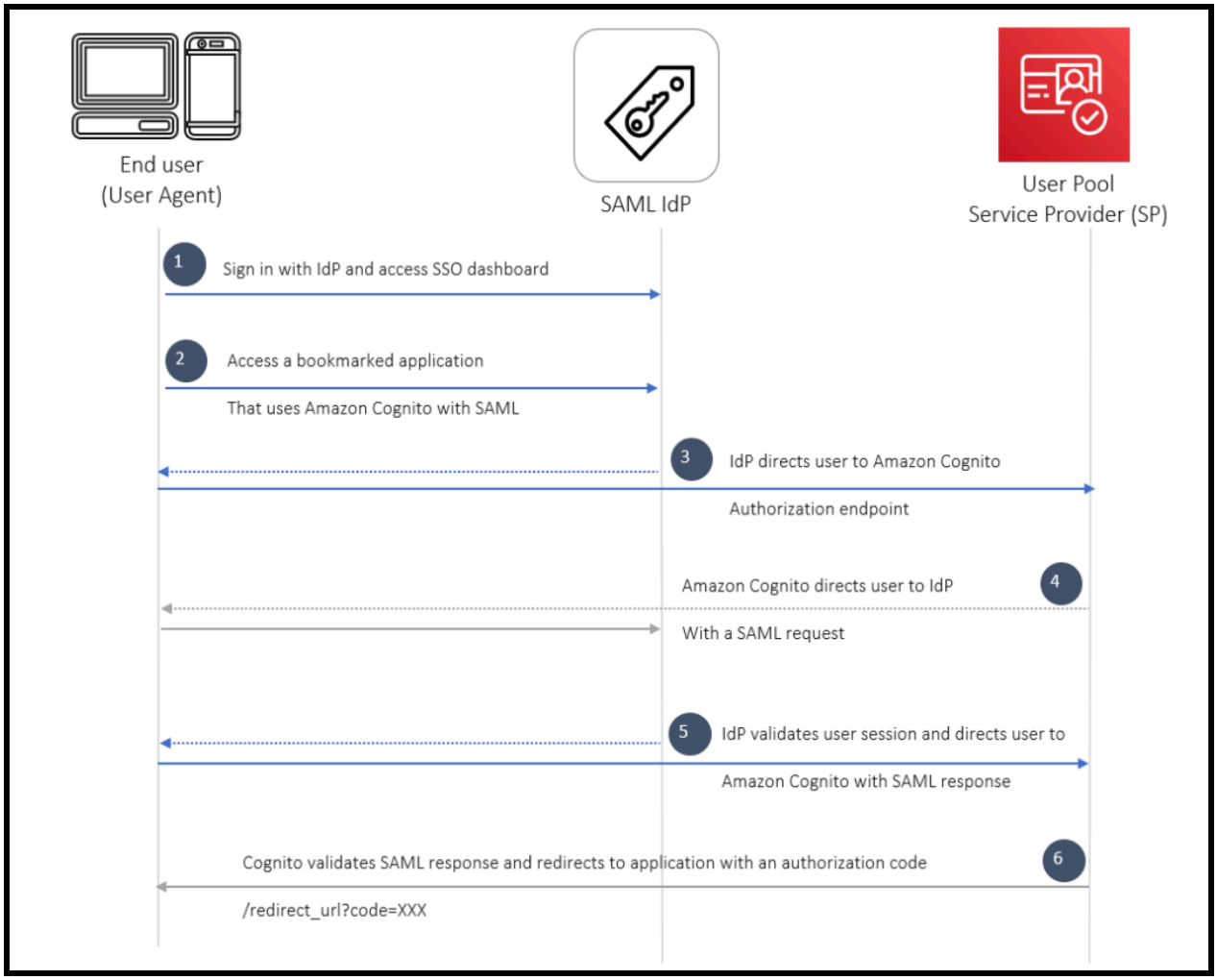

Figure 55. *Single Sign On (SSO) authentication flow with AWS Cognito User Pools. Setup by request for clients who wish to use a more streamlined process compared to basic authentication with Bearer Tokens.*

6 References

Abdullah, A.N., K. Kamarudin, S.M. Mamduh, A.H. Adom and Z.H.M. Juffry, 2020. Effect of environmental temperature and humidity on different metal oxide gas sensors at various gas concentration levels. 2nd. Joint Conf. on Green Engineering Tech & Appl. Computing, IOP Conf Series: Materials Science and Engineering, 864, 012152, doi:10.1088/1757-899X/864/1/012152.

Abdullah, A.N., K. Kamarudin, L.M. Kamarudin, A.H. Adom, S.M. Mamduh, Z.H.M. Juffry, and V.H. Bennetts, 2022. Correction model for metal oxide sensor drift caused by ambient temperature and humidity, Sensors, 22, 3301, https://doi.org/10.3390/s22093301.

Aldahafeeri, T., M-K. Tran, R. Vrolyk, M. Pope and M. Fowler, 2020. A review of methane gas detection sensors: Recent developments and future perspectives. Inventions, 5, 28; doi:10.3390/inventions5030028.

Angot, H., B. Blomquist, D. Howard and 20 others, 2022. Year-round trace gas measurements in the central Arctic during the MOSAiC expedition. Sci Data, 9: 723, 10.1038/s41597-022-01769-6.

Bane, S. and K. Tarasenko, 2024. Combustible gas detectors for home inspectors, Int. Assoc. of Certified Home Inspectors, https://www.nachi.org/gas-detectors.htm

Barchyn, T.E., C.H. Hugenholtz, T. Gough, C. Vollrath and M. Gao, 2023. Low-cost fixed sensor deployments for leak detection in North American upstream oil and gas: Operational analysis and discussion of a prototypical program. Elem Sci Anth, 11: 1. DOI: https://doi.org/10.1525/elementa.2023.00045.

Bastviken, D., Nygren, J., Schenk, J., Parellada Massana, R., and Duc, N. T., 2020. Technical note: Facilitating the use of low-cost methane (CH_4) sensors in flux chambers – calibration, data processing, and an open-source make-it-yourself logger, Biogeosciences, 17, 3659–3667, https://doi.org/10.5194/bg-17-3659-2020.

Bell, C., C. Ilonze, A. Duggan, and D. Zimmerle, 2023. Performance of continuous emission monitoring solutions under a single-blind controlled testing protocol. Environ. Sci. and Technol., 57, 5794-5805. (Included in Supplementary Materials).

Benko, T., A. MacGregor, E. Wen, T. Fox and B. Moorhouse, 2023. Continuous methane monitoring: Equivalency evaluation of regulator-approved alternative leak detection and repair program in Alberta, Canada. SPE 209973, SPE Annual Tech. Conference and Exhibition, Houston, TX, 3-5 Oct. 2022.

Bolton, David. “The Computation of Equivalent Potential Temperature.” *Atmospheric Physics Group, Imperial College, London, England*, vol. 108, 1980, p. 1047. *American Meteorological Society*, https://journals.ametsoc.org/view/journals/mwre/108/7/1520-0493_1980_108_1046_tcoept_2_0_co_2.xml?tab_body=pdf.

Brantley, H.L., E.D. Thoma, W.C. Squier, B.B. Guven, and D. Lyon, 2014. Assessment of methane emissions from oil and gas production pads using mobile measurements, Environ. Sci. Technolo., 48, 14508-14515.

Carrascal, M.D., M. Puigcerver and P. Puig, 1993. Sensitivity of Gaussian plume model to dispersion specifications. Theor. Appl. Climatol. 48, 147-157.

Caulton, D.R., Q. Li, E. Bou-Zeid, J.P. Fitts, L.M. Golston, D. Pan, L. Lu, H.M. Lane, B. Bucholz, X. Guo, J. McSpiritt, L. Wendt and M.A. Zondlo, 2018. Quantifying uncertainties from mobile-laboratory-derived emissions of well pads using inverse Gaussian methods. Atmos. Chem. Phys., 18, 15145-15168, https://doi.org/10.5914/acp-18-15145-2018.

Chai, H., Z. Zheng, K. Liu, J. Xu, K. Wu, Y. Luo, H. Liao, M. Debliquy and C. Zhang. 2022. Stability of metal oxide semiconductor gas sensors: A review. IEEE Sensors Journal, Vo. 22, No. 6, 5470-5481.

Collier-Oxandale, A., J.G. Casey, R. Piedrahita, J. Ortega, H. Halliday, J. Johnston, and M.P. Hannigan, 2018. Assessing a low-cost methane sensor quantification system for use in complex rural and urban environments. Atmos. Meas. Tech., 11, https://doi.org/10.5194/amt-11-3569-2018, pp. 3569-3594.

Dhall, S., B.R. Mehta, A.K. Tyagi, and K. Sood, 2021. A review on environmental gas sensors: Materials and technologies. Sensors International, Vol. 2, 100116.

Dlugokencky, E.J., L.P. Steele, P.M. Lang and K.A. Masarie, 1994. The growth rate and distribution of atmospheric methane. J. Geophys. Res., 99, 17,021– 17,043, doi:10.1029/94JD01245.https://doi.org/10.1029/94JD01245.

Earthview, 2022. Evaluating Earthview's methane detection under real-world conditions. Earthview White Paper #2022-2, 7 pp.

Edie, R., A.M. Robertson, R.A. Field, J. Soltis, D.A. Snare, D. Zimmerle, C.S. Bell, T.L. Vaughn and S.M. Murphy, 2020. Constraining the accuracy of flux estimates using OTM 33A. Atmos. Meas. Tech., 13, 341-353, https://doi.org/10.5194/amt-13-341-2020.

Eugster, W. and G.W. Kling, 2012. Performance of a low-cost methane sensor for ambient concentration measurements in preliminary studies. *Atmospheric Measurement Techniques* 5(8): 1925–1934. DOI: https://dx.doi.org/10.5194/amt-5-1925-2012.

Eugster, W., Laundre, J., Eugster, J., and Kling, G. W., 2020. Long-term reliability of the Figaro TGS 2600 solid-state methane sensor under low-Arctic conditions at Toolik Lake, Alaska, Atmos. Meas. Tech., 13, 2681–2695, https://doi.org/10.5194/amt-13-2681-2020.

Farrance, Ian, and Robert Frenkel. “Uncertainty in Measurement: A Review of Monte Carlo Simulation Using Microsoft Excel for the Calculation of Uncertainties Through Functional Relationships, Including Uncertainties in Empirically Derived Constants.” *The Clinical Biochemist*, vol. 35, no. 1, 2014, pp. 37-61. *National Library of Medicine*, https://www.ncbi.nlm.nih.gov/pmc/articles/PMC3961998/.

Figaro USA, 2021. Technical information for methane gas sensors. https://figarosensor.com/pdf/Figaro_USA_Sales_T&C.pdf

Finn, D., K.L. Clawson, R.M. Eckman, H. Liu, E.S. Russell, and Z. Gao, 2016. Project Sagebrush: Revisiting the value of the horizontal plume spread parameter sigma y. J. Appl. Met. Climatol., Vol. 55, 1305-1322.

Foster-Wittig, T.A., E.D. Thoma and J.D. Albertson. 2015. Estimation of point source fugitive emission rates from a single sensor time series: A conditionally-sampled Gaussian plume reconstruction. Atmos. Environ., 115, 101-109.

Fox, T.A., T.E. Barchyn, D. Risk, A.P. Ravikumar and C.H. Hugenholtz, 2018. A review of close-range and screening technologies for mitigating fugitive methane emissions in upstream oil and gas. Env. Res. Lett.14 (2019)053002, htts://doi.org/10.1088/1748-9326/ab0cc3.

Furuta, D., T. Sayahi, J. Li, B. Wilson, A.A. Presto, and J. Li, 2022. Atmos. Meas. Tech., Vol. 15, Issue 17, AMT. 15.5117-5128.

Glaessgen, E.H. and D.S. Stargel, 2012. The digital twin paradigm for future NASA and U.S. Air Force vehicles. 53rd. Structures, Structural Dynamics, and Materials Conf., Special Session on the Digital Twin, Am. Inst. Aeronautics and Astronautics.

Hanna, S.R., 2020. Letter to the editor on simple short range transport and dispersion (T&D) modeling of COVID-19 virus, indoors and outdoors, Journal of the Air & Waste Management Association, 70:10, 957-960, DOI: 10.1080/10962247.2020.1811611

Hanna, S.R., G.A. Briggs and R.P. Hosker, Jr., 1982. Handbook of atmospheric diffusion. DOE-TIC-11223, published by Technical Information Center, U.S. Dept. of Energy, 102 pp.

Helmig, D., 2020. Air quality impacts from oil and natural gas development in Colorado. Elem. Sci. Anth., 8: 4, DOI: https://doi.org/10.1525/elementa.398.

IBM, 2024. What is a digital twin? https://www.ibm.com/topics/what-is-a-digital-twin

Ilonze, C., E. Emerson, A. Duggan and D. Zimmler, 2024. Assessing the progress of the performance of continuous monitoring solutions under a single-blind controlled testing protocol. Env. Sci. and Tech., https://doi.org/10.1021/acs.est3c08511.

Irwin, J.S. and S.R. Hanna, 2005. Characterising uncertainty in plume dispersion models. Int. J. Env. and Pollution, Vol. 25, Nos. 1/2/3/4, 16-24.

Isaac, N.A., I. Pikaar, and G. Biskos, 2022. Metal oxide semiconducting nanomaterials for air quality gas sensors: operating principles, performance, and synthesis techniques. Microchimica Acta, 189:196, https://doi.org/10.1007/s00604-022-05254-0

Jacob, D.J., D.J. Varon, D.H. Cusworth and 12 others. 2022. Quantifying methane emissions from the global scale down to point sources using satellite observations of atmospheric methane. Atmos. Chem. Phys., 22, 9617-9646, https://doi.org/10.5194/acp-22-96177-2022.

Khalaf, W.M.H., 2012. Electronic nose system for safety monitoring at refineries. J. Eng. Dev., Vol. 16, No. 4, ISSN 1813-7822, 220-228.

Korsakissok, I. and V. Mallet, 2009. Comparative study of Gaussian dispersion formulas within the Polyphemus Platform: Evaluation with Prairie Grass and Kincaid experiments. J. Appl. Met. Climatol., vol. 48, 2459-2473.

Lines, I.G., D.M. Deaves, and W.S. Atkins, 1997. Practical modeling of gas dispersion in low wind speed conditions, for application in risk assessment. J. Hazardous Materials, 54, 201-226.

Lotrecchiano, N., D. Sofia, A. Guiliano, D. Barletta, and M. Poletto, 2020. Pollution dispersion from a fire using a Gaussian plume model. Int. J. Safety and Security Engineering, Vol. 10, No. 4, 431-439.

Maslanik, J.A., 2014. Evaluation of TTS air contaminants sensor package for remote, drive-by detection of methane release from oil/gas infrastructure, Earthview white paper WP-2014-1, 12 pgs. (See WP-2014-1 in Supplemental Materials).

Maslanik, J.A., 2021. An intercomparison of BluBird methane estimates with coincident high-accuracy observations obtained by an air quality monitoring site. Earthview white paper WP-2021-2 (See WP-2021-2 in Supplementary Materials), 12 pgs.

METEC, 2022. Continuous monitoring final report. ADED 2022 testing program – Performer: Earthview, 18 pp. (Included as CMReport_Earthview_v4_2022.pdf in Supplementary Materials).

METEC, 2024. Continuous monitoring final report. ADED 2024 testing program – Performer: Earthview, 21 pp. (Included as CMReport_Earthview_v3_2024.pdf in Supplementary Materials).

Miles, N.L., D.K. Martins, S.J. Richardson, C.W. Rella, C. Arata, T. Lauvaux, K.J. Davis, Z.R. Barkley, K. McKain and C. Sweeney, 2018. Calibration and field testing of cavity ring-down laser spectrometers measuring CH4, CO2, and s13 CH4 deployed on towers in the Marcellus Shale region, Atmos. Meas. Tech., 11, 1273-1295, https://www.cdc.gov/niosh/engcontrols/ecd/detail161.html

Moorhouse, B., B. Palma, and T. Fox, 2022. Qube Technologies continuous monitoring probability of detection: Results from independent single-blind controlled release testing. Highwood Emissions Management, Technical White Paper, August 2022, 12 pgs.

Papadopoulos, Christos, and Hoi Yeung. “Uncertainty estimation and Monte Carlo simulation method.” *Flow Measurement and Instrumentation*, vol. 12, no. 4, 2001, pp. 291-298. *Research Gate*,

https://www.researchgate.net/publication/223446790_Uncertainty_estimation_and_Monte_Carlo_simulation_method.

Pasquill, F., 1961. The Estimation of the Dispersion of Windborne Material. Meteorological Mag., 90, 33-49.

Pindado, Santiago, et al. “The Cup Anemometer, a Fundamental Meteorological Instrument for the Wind Energy Industry. Research at the IDR/UPM Institure.” *Sensors*, vol. 14, no.

11, 2014, pp. 21418-21452. *Research Gate*,

https://www.researchgate.net/publication/268281540_The_Cup_Anemometer_a_Fundamental_Meteorological_Instrument_for_the_Wind_Energy_Industry_Research_at_the_IDRUPM_Institute.

Possolo, A. et al., 2019. . “Asymmetrical Uncertainties.” *Metrologia*, vol. 56, no. 4, 2019. *IOP Science*,

https://iopscience.iop.org/article/10.1088/1681-7575/ab2a8d/meta.

Prabakaran, S. and J.B.B. Rayyapanan, 2015. Gas sensing mechanism of metal oxides; The role of ambient temperature, type of semiconductor and gases. A review. Sci Lett. J., 4, 1262015.

Riddick, S.N. , D.L. Mauzerall, M. Celia, G. Allen, J. Pitt, M. Kang and J.C. Riddick. 2020. The calibration and deployment of a low-cost methane sensor. Atmos. Environ., 230, 117440.

Riddick, S.N., R. Ancona, C.S. Bell, A. Duggan, T.L. Vaughn, K. Bennett, and D.J. Zimmerle, 2022a. Quantitative comparison of methods used to estimate methane emissions from small point sources. Atmos. Meas. Tech. Disc., DOI: https://doi.org/10.5194/amt-2022-9.

Riddick, S.N., R. Ancona, R. Cheptonui, C.S. Bell, A. Duggan, K.E. Bennett, and D.J. Zimmerle, 2022b. A cautionary report of calculating methane emissions using low-cost fence-line sensors Elementa: Science of the Anthropocene, 10 (1): 00021.

Robbiani, S., B.J. Lotesoriere, R.L. Dellaca, and L. Capelli, 2023. Physical confounding factors affecting gas sensors response: A review on effects and compensation strategies for electronic nose applications. Chemosensors, 11(10), 514; https://doi.org/10.3390/chemosensors11100514.

Robertson, A.M., R. Edie, D. Snare, J. Soltis, R.A. Field, M.D. Burkhart, C.S. Bell, D. Zimmerle and S.M. Murphy, 2017. Variation in methane emission rates from well pads in four oil and gas basins with contrasting production volumes and compositions. Environ. Sci. Technol., 51, 8832-8840.

Romain, A.C. and J. Nicolas, 2010. Long term stability of metal oxide-based gas sensors for e-nose environmental applications: An Overview. Sensors and Actuators, vol. 146, issue 2, pp. 502-506.

Sagendorf, J.F. and C.R. Dickson, 1974. Diffusion under low windspeed, inversion conditions. NOAA Tech. Memo. ERL, Air Resources Lab, ARL-52, 89 pp.

Schutze, A., T. Baur, M. Leidinger, W. Reimringer, R. Jung, T. Conrad, and Tilman Sauerwald, 2017. Highly sensitive and selective VOC sensor systems based on semiconductor gas sensors; How to? Environments, 4, 20, doi:10.3390/environments4010020.

Seiyama, T., A. Kato, Fujiishi, and K. Nagatani, 1962. A new detector for gaseous components using semiconductive thin films, Anal. Chem. 34, 1502-1503.

Shah, A., O. Laurent, L. Lienhardt, G. Broquet, R.R. Martinez, E. Allegrini, and P. Ciais. 2023. Characterizing the methane gas and environmental response of the Figaro Taguchi Gas Sensor (TGS) 2611-E00. Atmos. Meas. Tech., 16, 3391-3419, https://doi.org/10.5194/amt-16-3391-2003.

Sharan, M., A.K. Yadav, M.P. Singh, P. Agarwal and S. Nigam, 1996. A mathematical model for the dispersion of air pollutants in low wind conditions. Atmos. Environ., Vol. 30, No. 8, 1209-1220.

Sohn, J.H., M. Atzeni, L. Zeller, and G. Pioggia, 2007. Characterization of humidity dependence of a metal oxide semiconductor sensor array using partial least squares. Sensors and Actuators B, 131, pp 230-235.

Thome, K.J. and S. Tsuchida, 2008. Vicarious calibration of ASTER via the reflectance-based approach. IEEE Trans. Geosci. and Rem. Sens., 46(10), 3285-3295, DOI:10.1109/TGRS.2008.928730.

Torres, V.M., D.W. Sullivan, E. He'Bert, J. Spinhirne, M. Modi and D.T. Allen, 2022. Field inter-comparison of low-cost sensors for monitoring methane emissions from oil and gas production operations. Atmos. Meas. Tech., https://doi.org/10.5194/amt-2022-24.

Turner, D.B., 1970. Workbook of atmospheric dispersion estimates. Environmental Protection Agency, Office of Air Programs, 69 pp. (available from National Service Center for Environmental Publications.

Turner, A.J., C. Frankenberg and E.A. Kort, 2019. Interpreting contemporary trends in atmospheric methane. PNAS, 116 (8), 2805-2813, https://doi.org/10.1073/pnas.1814297116.

U.S. EPA, 2013. Standard operating procedures for analysis of US EPA geospatial measurement of air pollution - Remote emission quantification by direct assessment (GMAP-REQ-DA), SOP 601 for OTM 33A, US EPA Office of Research and Development.

U.S. EPA, 2014. Other Test Method (OTM) 33 and 33A Geospatial Measurement of air Pollution - Remote Emissions Quantification Direct Assessment (GMAP-REQ-DA), 91 pgs.

Van den Bossche, M., N.T. Rose, S.F.J. De Wekker, 2017. Potential of a low-cost gas sensor for atmospheric methane monitoring. Sensors and Actuators B: Chemical, 238, 501-509, https://doi.org/10.1016/snb.2016.07.092.

Vasiliev, A.A., A. E. Varfolomeev, I.A. Volkov, N.P. Sinonenko,, P.V. Arsenov, I.S. Vlasov, V.V. Ivanov, A.V. Pislyakov, A.S. Lagutin, I.E. Jahatspanian and T. Maeder. 2018. Reducing humidity response of gas sensors for medical applications: Use of spark discharge synthesis of metal oxide nanoparticles. Sensors, 18, 2600; doi:10.3390/s18082600, 13 pgs.

Wang, C., L. Yin, L. Zhang, D. Xiang and R. Gao, 2010. Metal oxide gas sensors: sensitivity and influencing factors. Sensors, 10(3): 2088-2106.

Wang, Y. and Y. Zhou, 2022. Progress on anti-humidity strategies of chemiresistive gas sensors. Materials, 15, 8728. https://doi.org/10.3390/ma15248728.

Xiong, X., J. Sun, W. Barnes, V. Salomonson, J. Esposito, H. Erives, and B. Guenther, 2007. Multiyear on-orbit calibration and performance of Terra MODIS reflective solar bands, *IEEE Trans. Geosci. Remote Sens.*, 45(4), April.

Yan, M.; Y. Wu, Z. Hua, N. Lu, W. Sun, J. Zhang and S. Fan, 2021. Humidity compensation based on power-law response for MOS sensors to VOCs. Sens. Actuators B Chem. 2021, 334, 129601.

Yang, M., Prytherch, J., Kozlova, E., Yelland, M. J., Parenkat Mony, D., and Bell, T. G., 2016. Comparison of two closed-path cavity-based spectrometers for measuring air–water CO_2 and CH_4 fluxes by eddy covariance, Atmos. Meas. Tech., 9, 5509–5522, https://doi.org/10.5194/amt-9-5509-2016.

Zibordi, G., F. Melin, K.J. Voss, B.C. Johnson, B.A. Franz, E. Kwiatkowska, J-P. Huot, M. Wang and D. Antoine, 2015. System vicarious calibration for ocean color climate change applications: Requirements for in situ data. Rem. Sens. Env. Vol. 159, 361-369. https://doi.org/10.1016/j.rse.2014.12.015